spectra were searched against the nonredundant protein sequence database maintained at the National Center for Biotechnology Information using the Mascot program (Matrixscience) to identify proteins. The MS/MS signal assignments were also confirmed manually.

Expression and purification of recombinant proteins. *E. coli* BL21(DE3) cells were transformed with plasmids expressing GST fusion protein or His-tagged protein and grown at 37°C. Expression of the fusion protein was induced by 1 mM isopropyl-β-D-thiogalactopyranoside at 37°C for 4 h. Bacteria were harvested, suspended in lysis buffer (phosphate-buffered saline [PBS] containing 1% Triton X-100), and sonicated on ice.

Hi5 cells were infected with recombinant baculoviruses to produce GST-C173HT, GST-C152HT, GST-HT, MEF-E6AP, and His-tagged mouse E1 (17). GST and GST fusion proteins were purified on glutathione-Sepharose beads (Amersham Bioscience) according to the manufacturer's protocols. His-tagged proteins were purified on nickel-nitrilotriacetic acid beads (QIAGEN) according to the manufacturer's protocols. MEF-E6AP and MEF-E6AP C-A were purified on anti-FLAG M2 agarose beads (Sigma) according to the manufacturer's protocols.

Immunoblot analysis. Immunoblot analysis was performed essentially as described previously (11). The membrane was visualized with SuperSignal West Pico chemiluminescent substrate (Pierce).

HCV core protein and E6AP binding assays. To map the E6AP binding site on HCV core protein, 2.5 μg of purified recombinant GST-E6AP expressed in Hi5 cells was mixed with 1,000 μg of 293T cell lysates transfected with a series of FLAG-tagged HCV core deletion mutants as indicated. The protein concentration of the cells was determined using the bicinchoninic acid protein assay kit (Pierce). The mixtures were immunoprecipitated with anti-FLAG M2 agarose beads (Sigma), and proteins bound to the immobilized HCV core protein on anti-FLAG beads were dissociated with FLAG peptide (Sigma). The eluates were analyzed by immunoblotting with anti-GST PAb. To map the HCV core-binding site on E6AP, GST pull-down assays were performed as described previously (51).

In vivo ubiquitylation assay. In vivo ubiquitylation assays were performed essentially as described previously (57). FLAG-core was immunoprecipitated with anti-FLAG beads. Immunoprecipitates were analyzed by immunoblotting, using either anti-HA PAb or anticore PAb (TS1) to detect ubiquitylated core proteins.

In vitro ubiquitylation assay. For in vitro ubiquitylation of HCV core protein, purified GST-C173HT and GST-C152HT were used as substrates. Purified GST-HT was used as a negative control. Assays were done in 40-μl volumes containing 20 mM Tris-HCl, pH 7.6, 50 mM NaCl, 5 mM ATP, 10 mM $MgCl_2$, 8 μg of bovine ubiquitin (Sigma), 0.1 mM dithiothreitol, 200 ng mouse E1, 200 ng E2 (UbcH7), and 0.5 μg each of MEF-E6AP or MEF-E6AP C-A. The reaction mixtures were incubated at 37°C for 120 min followed by purification with glutathione-Sepharose beads and immunoblotting with the indicated antibodies.

siRNA transfection. 293T cells or Huh-7 cells at 3×10^5 cells in a six-well plate were transfected with 40 pmol of either E6AP-specific short interfering RNA (siRNA; Sigma) or scramble negative-control siRNA duplexes (Sigma) using HiPerFect transfection reagent (QIAGEN) following the manufacturer's instructions. The siRNA target sequences were as follows: E6AP (sense), 5′-GGGUC UACACCAGAUUGCUTT-3′; scramble negative control (sense), 5′-UUGCG GGUCUAAUCACCGATT-3′.

CHX half-life experiments. To examine the half-life of HCV core protein, transfected 293T cells were treated with 50 μg/ml cycloheximide (CHX) at 44 h posttransfection. The cells at zero time points were harvested immediately after treatment with CHX. Cells from subsequent time points were incubated in medium containing CHX at 37°C for 3, 6, and 9 h as indicated.

Infection of Huh-7 cells with secreted HCV. Infectious HCV JFH1 was produced in Huh-7.5.1 cells (61) as described previously (56). Culture supernatant containing infectious HCV JFH1 was collected and passed through a 0.22-μm filter. Naïve Huh-7 cells were seeded 24 h before infection at a density of 1×10^6 in a 10-cm dish. The cells were incubated with 2.5 ml of the inoculum (6.5×10^3 50% tissue culture infectious dose [$TCID_{50}$]/ml) for 3 h, washed three times with PBS, and supplemented with fresh complete Dulbecco's modified Eagle's medium. Then the cells were transfected with 6 μg each of pCAGGS, pCAG-HA-E6AP, or pCAG-HA-E6AP C-A by using TransIT LT1 (Mirus). The cells were trypsinized and replated in six-well plates at 1 day postinfection. The culture medium was changed every 2 days. The culture supernatants and the cells were collected at days 3 and 7 postinfection.

Quantitation of HCV RNA and core protein. We quantitated HCV core protein in cell lysate using the HCV core antigen enzyme-linked immunosorbent assay (ELISA) (Ortho-Clinical Diagnostics). Total RNA was extracted from cells using TRIzol reagent (Invitrogen). To quantitate HCV RNAs, real-time reverse transcription-PCR was performed as described previously (53).

Infectivity assay. The $TCID_{50}$ was calculated essentially based on the method described previously (28). Virus titration was performed by seeding Huh-7 cells in 96-well plates at 1×10^4 cells/well. Samples were serially diluted fivefold in complete growth medium and used to infect the seeded cells (six wells per dilution). Following 3 days of incubation, the cells were immunostained for core with anticore MAb (2H9). Wells that expressed at least one core-expressing cell were counted as positive, and the $TCID_{50}$ was calculated.

Immunocytochemistry and fluorescence microscopy. Cells on collagen-coated coverslips were washed with PBS, fixed with 4% paraformaldehyde for 30 min at 4°C, and permeabilized with PBS containing 0.2% Triton X-100. Cells were preincubated with BlockAce (Dainippon Pharmaceuticals), incubated with specific antibodies as primary antibodies, washed, and incubated with rhodamine-conjugated goat anti-rabbit immunoglobulin G (ICN Pharmaceuticals, Inc.) and Qdot 565-conjugated goat anti-mouse immunoglobulin G (Quantumdot) as secondary antibody. Then the cells were washed with PBS, counterstained with DAPI (4′,6′-diamidino-2-phenylindole) solution (Sigma) for 3 min, mounted on glass slides, and examined with a BZ-8000 microscope (Keyence).

Knockdown of endogenous E6AP in HCV JFH1-infected Huh-7 cells. Naïve Huh-7 cells at 10^6 cells/10-cm dish were inoculated with 2.5 ml of the inoculum including infectious HCV JFH1 (6.5×10^3 $TCID_{50}$/ml) and cultured. The cells were replated in a six-well plate at 3×10^5 cells/well at day 11 postinfection and transfected with 40 pmol of E6AP siRNA or control siRNA. The culture medium was changed at 24 h after transfection. The cells were harvested at day 2 after transfection, and the intracellular core protein levels were quantitated using the HCV core antigen ELISA. The culture supernatants were collected at day 2 after transfection and assayed for $TCID_{50}$ determinations.

RESULTS

Identification of E6AP as an HCV core-binding protein. To identify the molecular machinery for HCV core ubiquitylation, we searched for endogenous ubiquitin-proteasome pathway proteins that associated with HCV core protein. HCV core-binding proteins (i.e., MEF core and its binding proteins, recovered from lysed cells) were purified by a tandem affinity purification procedure using a tandem tag (known as MEF tag) (16). Ten proteins were reproducibly detected (Fig. 1A, lane 2), but none were recovered from lysed control cells transfected with empty vector alone (Fig. 1A, lane 1).

To identify the proteins, silver-stained bands were excised from the gel, digested by Lys-C, and analyzed using a direct nanoflow liquid chromatography-MS/MS system. Nine proteins were identified: two known HCV core-binding proteins, human DEAD box protein DDX3 (38) and proteasome activator PA28γ (30), and seven potential HCV core-binding proteins. E6AP was identified (Fig. 1A, lane 2) on the basis of five independent MS/MS spectra (Table 1). Immunoblot analyses confirmed the proteomic identification of E6AP, DDX3, PA28γ, and MEF-core (Fig. 1B to E).

E6AP binding domain for HCV core protein. The E6AP binding domain for HCV core protein was investigated. Figure 2A is a schematic representation of E6AP and known motifs in E6AP. A series of deletion mutants of E6AP as GST fusion proteins were expressed in *E. coli*. GST pull-down assays found that the carboxyl-terminal deletion mutant E6AP (1–517), but not E6AP (1–418) (Fig. 2C, lanes C and D), and the amino-terminal deletion mutant E6AP (418–875), but not E6AP (517–875) (Fig. 2C, lanes J and K), were able to bind to the core protein. The signal was absent when unprogrammed wheat germ extracts (the negative control) were used as a source of proteins (data not shown). GST pull-down assays (Fig. 2B) found that the region from aa 418 to aa 517 is important for binding to the HCV core protein. An assay of the

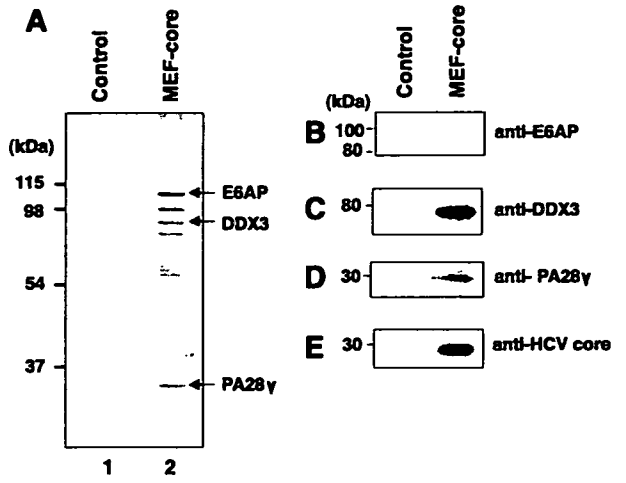

FIG. 1. HCV core protein associates with E6AP in vivo. (A) 293T cells were transfected with pcDNA3-MEF-core or empty plasmid, incubated for 48 h, and then harvested. The expressed MEF-core and binding proteins were recovered using the MEF purification procedure. Proteins bound to the MEF-core immobilized on anti-FLAG beads were dissociated with FLAG peptides, resolved by 9% SDS-PAGE, and visualized by silver staining. Control experiments were performed using 293T cells transfected with vector alone. The positions of E6AP, DDX3, and PA28γ are indicated by arrows. (B to E) The proteins detected in panel A were confirmed by immunoblotting with appropriate antibodies: E6AP (B), DDX3 (C), PA28γ (D), and MEF-core (E).

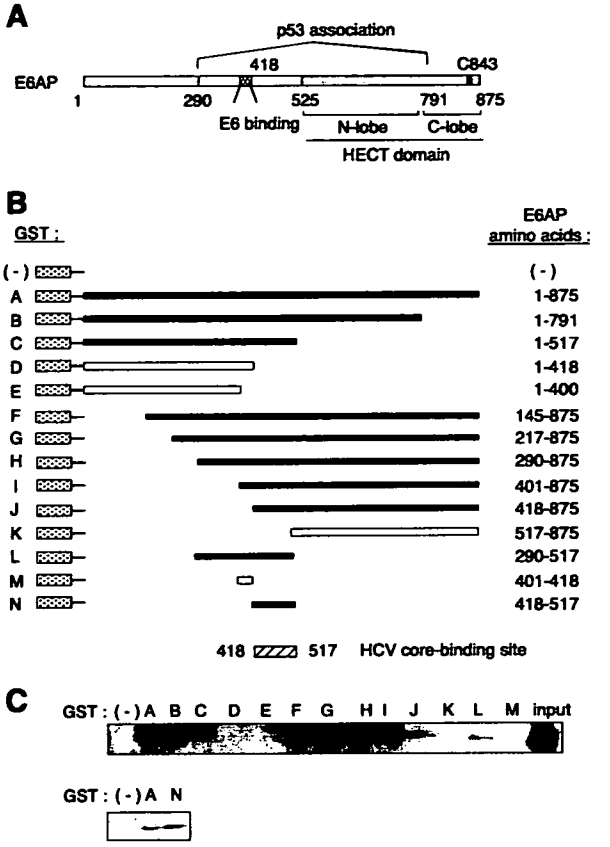

FIG. 2. Mapping of the HCV core-binding domain for E6AP. (A) Structure of E6AP. Shown is a schematic representation of the regions of E6AP isoform II that mediate E6 binding (aa 401 to 418), E6-dependent association with p53 (aa 290 to 791), and the HECT catalytic domain (aa 525 to 875). The catalytic cysteine residue is located at aa 843. (B) Schematic representation of GST-E6AP proteins. GST proteins A through N contain the E6AP amino acids indicated to the right. The shaded region of each represents the GST sequence. Closed boxes represent proteins that are bound specifically to HCV core protein, and open boxes represent those that are not bound. (C) Binding of HCV core protein to GST-E6AP proteins A through N. In vitro-translated core protein (aa 1 to 173) was assayed for association with GST (-) or the GST-E6AP fusion proteins A through N. Association of core protein was detected by immunoblotting with anti-core MAb.

ability of GST-E6AP (418–517) to bind to the HCV core protein was confirmatory (Fig. 2C, lane N) and led to the conclusion that the HCV core-binding domain of E6AP was aa 418 to aa 517.

The HCV core-binding domain for E6AP. By use of a panel of HCV core deletion mutants (Fig. 3A), GST-E6AP was found to coimmunoprecipitate with all of the FLAG-core proteins (Fig. 3A, lanes A to H) except FLAG-core (72–191) or FLAG-core (92–191) (Fig. 3A, lanes I and J). No association of control GST protein with any FLAG-core proteins was observed (data not shown). These data suggest that the aa-58-to-aa-71 segment of the HCV core binds to E6AP. The ability of GST-core (58–71) to associate with purified MEF-E6AP confirmed that the core (aa 58–71) was the site for E6AP binding on the HCV core protein (Fig. 3B).

E6AP decreases steady-state levels of HCV core protein in 293T cells and HepG2 cells. One of the features of HECT domain ubiquitin ligases is direct association with their substrates (50). Thus, we hypothesized that E6AP would function as an E3 ubiquitin ligase for the HCV core protein. We assessed the effects of E6AP on the HCV core protein in 293T cells. FLAG-core (1–191) together with HA-tagged wild-type E6AP, catalytically inactive mutant E6AP, E6AP C-A (19), or WWP1 (another HECT domain ubiquitin ligase) (22) was introduced into 293T cells, and the levels of the core protein were examined by immunoblotting. The steady-state levels of the core protein decreased with an increase in the amount of E6AP plasmids (Fig. 4A and B). However, neither E6AP C-A mutant nor WWP1 decreased the steady-state levels of the core protein, suggesting that E6AP enhances degradation of the core protein.

To verify the critical need for endogenous E6AP in the core degradation, expression of E6AP was knocked down by siRNA and the expression of the core protein and E6AP was assayed by immunoblotting. Transfection of the E6AP-specific siRNA

TABLE 1. Identification of E6AP by tandem mass spectrometry[a]

Peptide *m/z*	Sequence determined	Residues
720.9	VFSSAEALVQSFR	156–168
922.4	AACSAAAMEEDSEASSSR	196–213
774.9	MMETFQQLITYK	339–350
1,053.1	ITVLYSLVQGQQLNPYLR	507–524
809.4	EFVISYSDYILNK	712–724

[a] The protein was ubiquitin protein ligase E3A (E6AP) isoform 2 (GenBank accession no. NP_000453).

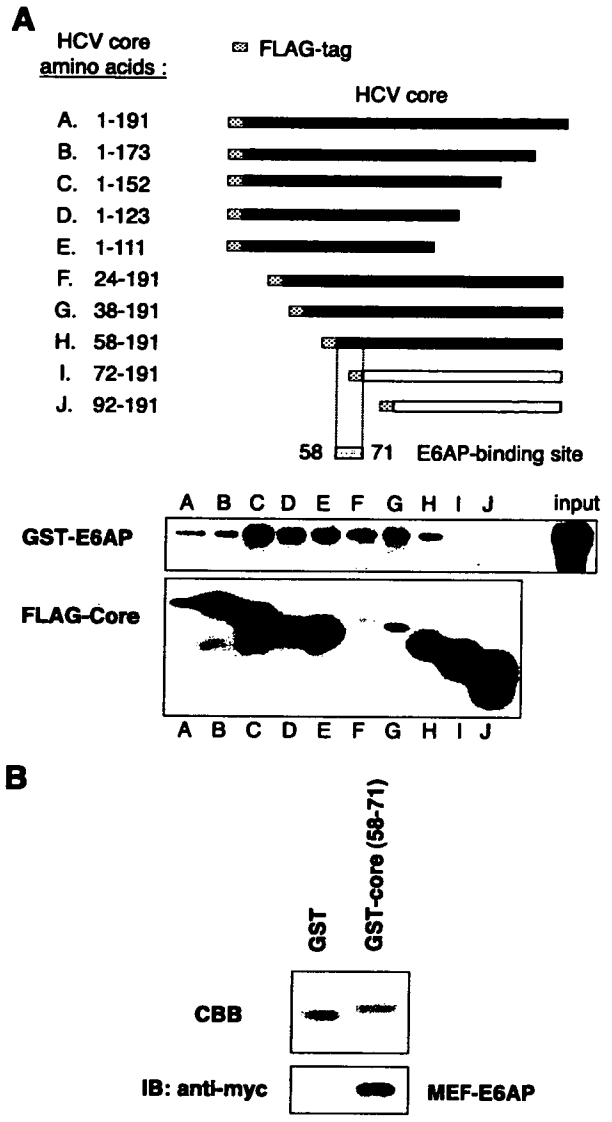

FIG. 3. Mapping of the E6AP binding domain for HCV core protein. (A) In vitro binding of E6AP to HCV core protein. 293T cells were transfected with each plasmid indicated in the upper panel. At 48 h posttransfection, cell lysates were mixed with purified GST-E6AP, immunoprecipitated with anti-FLAG beads, and then immunoblotted with anti-GST PAb (middle panel) or anti-FLAG MAb (bottom panel). The last lane (input) represents GST-E6AP used in this assay (middle panel). (B) Binding of GST-core (aa 58 to aa 71) to purified MEF-E6AP. GST served as a negative control for binding. Upper panel, Coomassie blue-stained SDS-PAGE of GST and GST-core (58–71). Lower panel, results of the GST pull-down assay. MEF-E6AP was detected by anti-myc MAb. CBB, Coomassie brilliant blue; IB, immunoblot.

duplex reduced the protein level of E6AP by 90% at 48 h posttransfection (Fig. 4C, middle panel). Immunoblotting revealed a 4.1-fold increase in the level of the core protein in the cells transfected with E6AP siRNA (Fig. 4C, top panel), suggesting that endogenous E6AP plays a role in the proteolysis of the HCV core protein.

Then we examined whether E6AP reduces the steady-state

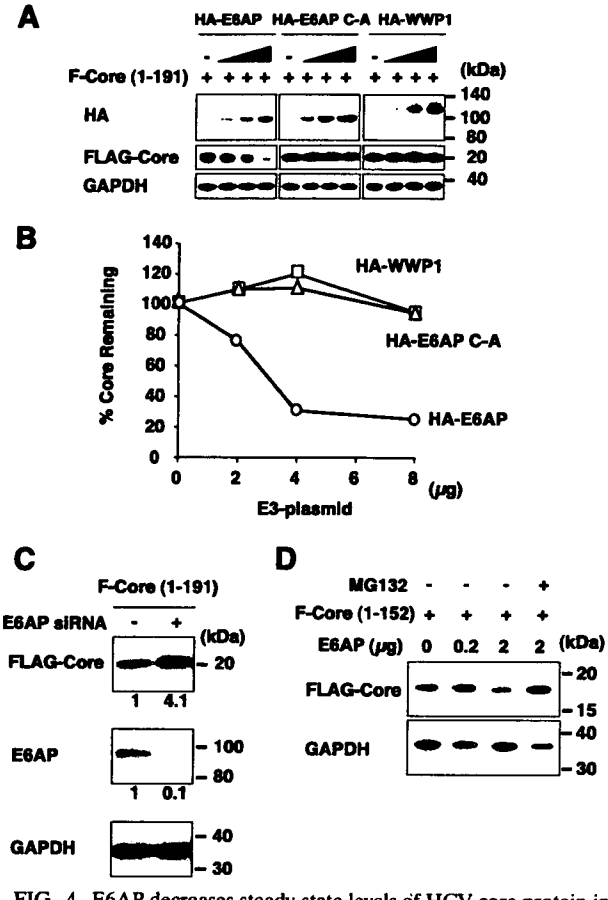

FIG. 4. E6AP decreases steady-state levels of HCV core protein in 293T cells and in HepG2 cells. (A) 293T cells (1×10^6 cells/10-cm dish) were transfected with 1 μg of pCAG FLAG-core (1–191) along with either pCAG-HA-E6AP, pCAG-HA-E6AP C-A, or pCAG-HA-WWP1 as indicated. At 48 h posttransfection, protein extracts were separated by SDS-PAGE and analyzed by immunoblotting with anti-HA PAb (top panel), anti-FLAG MAb (middle panel), and anti-GAPDH MAb (bottom panel). (B) Quantitation of data shown in panel A. Intensities of the gel bands were quantitated using the NIH Image 1.62 program. The level of GAPDH served as a loading control. Circles, E6AP; triangles, E6AP C-A; squares, WWP1. (C) Knockdown of endogenous E6AP by siRNA inhibits degradation of HCV core protein in 293T cells. 293T cells (3×10^5 cells/six-well plate) were transfected with 40 pmol of E6AP-specific duplex siRNA (or control siRNA) as described in Materials and Methods. The cells were transfected with 2 μg of FLAG-core (1–191) expression plasmid and cultured for 24 h, harvested, and analyzed by immunoblotting. Shown is immunoblot detection of FLAG-tagged core protein (top panel), E6AP protein (middle panel), and GAPDH (bottom panel) in control siRNA-treated 293T cells or E6AP-siRNA-treated 293T cells. The relative levels of protein expression were quantitated by densitometry and indicated below in the respective lanes. GAPDH served as a loading control. (D) HepG2 cells (2×10^5 cells/six-well plate) were transfected with pCAG FLAG-core (1–152) along with either empty vector or pCMV E6AP as indicated. The cells were harvested at 44 h posttransfection. Where indicated, cells were treated with 25 μM MG132 or with dimethyl sulfoxide control 14 h prior to collection. Equivalent amounts of the whole-cell lysates were separated by SDS-PAGE and analyzed by immunoblotting with anti-FLAG MAb (upper panel) or anti-GAPDH MAb (lower panel).

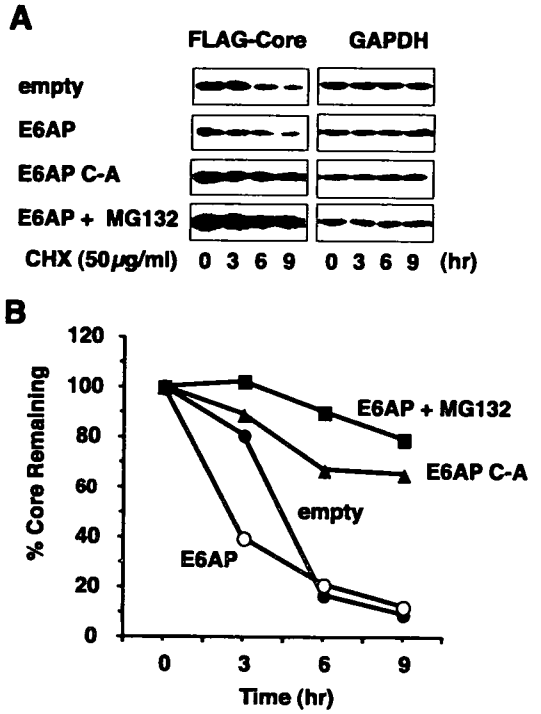

FIG. 5. Kinetic analysis of E6AP-dependent degradation of HCV core protein. (A) 293T cells (1×10^6 cells/10-cm dish) were transfected with 1 μg of pCAG-FLAG core (1–152) plus 4 μg of empty vector, pCMV-HA-E6AP, or pCMV-HA-E6AP C-A. The cells were treated with 50 μg/ml CHX at 44 h after transfection. Cell extracts were collected at 0, 3, 6, and 9 h after treatment with CHX, followed by immunoblotting. (B) Specific signals were quantitated by densitometry, and the percent remaining core at each time was compared with that at the starting point. The level of GAPDH served as a loading control. Open circles, E6AP; closed circles, empty plasmid; closed triangles, E6AP C-A; closed squares, E6AP with MG132 treatment. Data are representative of three independent experimental determinations.

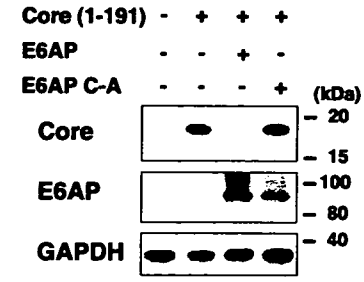

FIG. 6. E6AP promotes degradation of full-length HCV core protein in Huh-7 cells. Huh-7 cells (2×10^5 cells/six-well plate) were transfected with 0.5 μg of pCAG-core (1–191) together with 2 μg of pCMV-HA-E6AP or pCMV-HA-E6AP C-A. At 48 h posttransfection, cells were harvested and analyzed by immunoblotting with anticore MAb (top panel), anti-E6AP PAb (middle panel), or anti-GAPDH MAb (bottom panel).

levels of the core protein in hepatic cells as well as in 293T cells. Exogenous expression of E6AP resulted in reduction of the core protein in human hepatoblastoma HepG2 cells (Fig. 4D). Treatment of the cells with the proteasome inhibitor MG132 increased the core protein level, suggesting that the core protein was degraded through the ubiquitin-proteasome pathway. These results indicate that E6AP enhances proteasomal degradation of the HCV core protein in both hepatic cells and nonhepatic cells.

Kinetic analysis of E6AP-dependent degradation of HCV core protein. To determine whether the E6AP-induced reduction of the core protein is due to an increase in the rate of core degradation, we performed kinetic analysis using the protein synthesis inhibitor CHX. HCV core protein together with wild-type E6AP or inactive mutant E6AP C-A was expressed in 293T cells. At 44 h after transfection, cells were treated with either 50 μg/ml CHX alone or 50 μg/ml CHX plus 25 μM MG132 to inhibit proteasome function. Cells were collected at 0, 3, 6, and 9 h following treatment and analyzed by immunoblotting (Fig. 5A). Overexpression of E6AP resulted in rapid degradation of the core protein, whereas inactive mutant E6AP C-A increased the half-life of the core protein (Fig. 5B), suggesting that the inactive E6AP inhibited degradation of the core protein in a dominant-negative manner, which is in agreement with previous studies (19, 55). Treatment of the cells with MG132 inhibited the degradation of the core protein (Fig. 5B). Reverse transcription-PCR to determine mRNA levels of the HCV core gene and GAPDH gene found that neither wild-type E6AP nor inactive E6AP changed mRNA levels of the HCV core gene and GAPDH gene (data not shown). These results indicate that E6AP enhances proteasomal degradation of the core protein.

E6AP promotes degradation of the full-length core protein in Huh-7 cells. To determine whether the full-length HCV core protein expressed in hepatic cells is degraded through an E6AP-dependent pathway, human hepatoma Huh-7 cells were transfected with pCAG HCV core (1–191) along with either E6AP or E6AP C-A. To rule out the effects of N-terminal FLAG tag on the core degradation, HCV core protein was expressed as untagged protein. Expression of wild-type E6AP resulted in reduction of the core protein (Fig. 6). On the other hand, HCV core protein was not decreased after transfection of inactive E6AP, indicating that the full-length core protein expressed in Huh-7 cells is also degraded through an E6AP-dependent pathway.

E6AP mediates ubiquitylation of HCV core protein in vivo. To determine whether E6AP can induce ubiquitylation of HCV core protein in cells, we performed in vivo ubiquitylation assays. 293T cells were cotransfected with FLAG-core (1–191) and either E6AP or empty plasmid, together with a plasmid encoding HA-tagged ubiquitin to facilitate detection of ubiquitylated core protein. Cell lysates were immunoprecipitated with anti-FLAG MAb and immunoblotted with anti-HA PAb to detect ubiquitylated core protein (Fig. 7A). Only a little ubiquitin signal was observed on the core protein in the absence of cotransfected E6AP (Fig. 7A, lane 3). In contrast, coexpression of E6AP led to readily detectable ubiquitylated forms of the core protein as a ladder and a smear of higher-molecular-weight bands (Fig. 7A, compare lane 3 with lane 4). Immunoblot analysis with anticore PAb confirmed that FLAG-core proteins were immunoprecipitated (Fig. 7B, lanes 2 to 4, short exposure) and that higher-molecular-weight bands con-

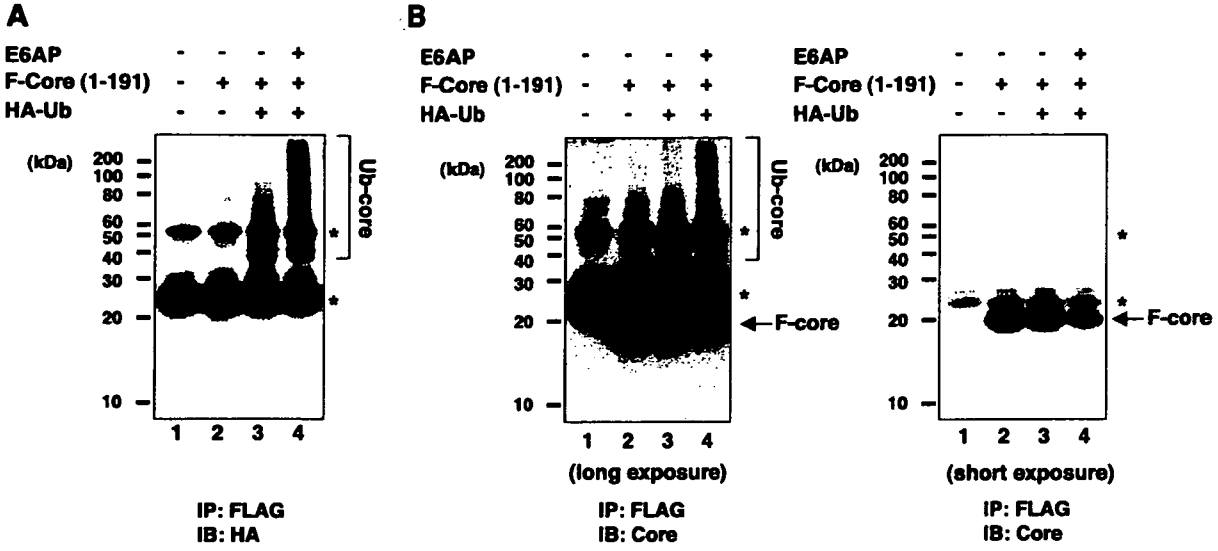

FIG. 7. E6AP-dependent ubiquitylation of HCV core protein in vivo. 293T cells (1×10^6 cells/10-cm dish) were transfected with 1 μg of pCAG FLAG-core (1–191) together with 2 μg of plasmid encoding E6AP as indicated. Each transfection also included 2 μg of plasmid encoding HA-ubiquitin. The cell lysates were immunoprecipitated with FLAG beads and analyzed by immunoblotting with anti-HA PAb (A) or anticore PAb (B). A shorter exposure of the core blot shows immunoprecipitated FLAG-core protein (B, right panel). A longer exposure of the core blot shows the presence of a ubiquitin smear (B, left panel). Asterisks indicate cross-reacting immunoglobulin light chain or heavy chain. Arrows indicate FLAG-core. IB, immunoblot; IP, immunoprecipitation.

jugated with HA-ubiquitin were indeed ubiquitylated forms of the core protein (Fig. 7B, lanes 3 and 4, long exposure).

E6AP mediates ubiquitylation of HCV core protein in vitro. To rule out the possibility that E6AP contributes to core protein degradation by inducing degradation of inhibitors of core turnover, we determined whether E6AP functions directly as a ubiquitin ligase by testing the ability of purified MEF-E6AP to mediate in vitro ubiquitylation of the purified recombinant HCV core protein. HCV core protein was expressed as a fusion protein containing N-terminal GST tag and C-terminal His tag and purified as described in Materials and Methods. GST-C173HT (aa 1–173) and GST-C152HT (aa 1–152) (see Materials and Methods) were used to determine whether the mature core protein and the C-terminally truncated core protein are targeted for ubiquitylation in vitro. The validity of this assay was established by demonstrating that E6AP but not E6AP C-A induced ATP-dependent ubiquitylation of GST-core protein. When in vitro ubiquitylation reactions were carried out either in the absence of MEF-E6AP or in the presence of MEF-E6AP C-A, no ubiquitylation signal was detected (Fig. 8A, lanes 4 and 5). However, inclusion of purified MEF-E6AP in the reaction mixture resulted in marked ubiquitylation of GST-C173HT (Fig. 8A, lane 6), while no ubiquitylation was observed in the absence of ATP (Fig. 8A, lane 7). No signal was detected when GST-HT was used as a substrate (Fig. 8A, lane 8). The higher-molecular-weight species of GST-core proteins were reactive with both anti-ubiquitin MAb (Fig. 8B, right panel, lanes 2 and 4) and anti-GST MAb (Fig. 8B, left panel, lanes 2 and 4). Both GST-C152HT and GST-C173HT were polyubiquitylated by E6AP in vitro (Fig. 8B), indicating that both the C-terminally truncated core and the mature core are polyubiquitylated by E6AP in vitro. These results revealed that E6AP directly mediated ubiquitylation of HCV core proteins in an ATP-dependent manner.

Exogenous expression of E6AP reduces intracellular HCV core protein levels and supernatant infectivity titers in HCV-infected Huh-7 cells. We used a recently developed system for the production of infectious HCV particles using the HCV JFH1 strain (28, 56, 61) to examine whether E6AP can promote degradation of HCV core protein expressed from infectious HCV. E6AP-dependent core degradation was assessed in Huh-7 cells inoculated with the culture supernatant containing HCV JFH1. Levels of HCV core protein were detectable at day 3 postinfection and increased with time. Immunofluorescence staining for the core protein indicated that the percentage of HCV core-positive cells in the Huh-7 cells was almost 100 at day 7 postinfection. Transfection efficiency was 50 to 60% as measured with GFP-expressing plasmid. At day 7 postinfection, exogenous expression of E6AP reduced the intracellular core protein level by about 60% compared to the empty plasmid-transfected control cells (Fig. 9A). Inactive E6AP had little effect on the core protein levels. Total protein levels in the cells (Fig. 9B) and intracellular HCV RNA levels (Fig. 9C) did not change after transfection of wild-type E6AP or inactive E6AP. The immunofluorescence study revealed that HCV core protein was variably detected and the intensity of core staining was reduced in the cells staining positive for wild-type E6AP compared with neighboring cells staining negative for E6AP (Fig. 9E). Using inactive E6AP revealed colocalization of the core protein and E6AP in the perinuclear region (Fig. 9F) of HCV-infected cells. These results suggest that E6AP enhanced degradation of HCV core protein expressed from infectious HCV. Then we titrated HCV infectivity in the culture supernatant at day 7 postinfection by limiting

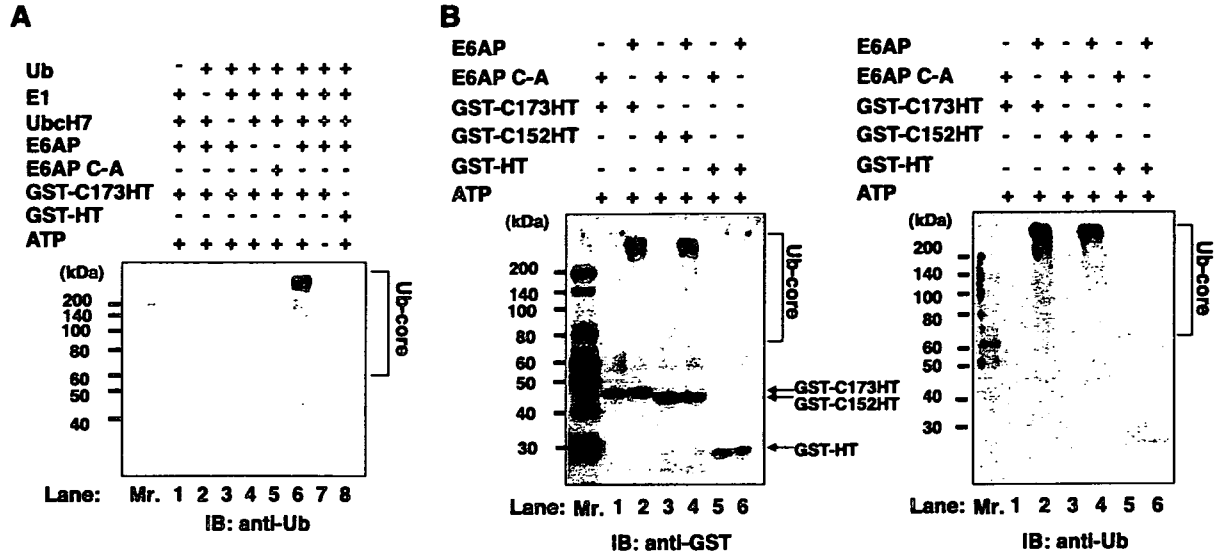

FIG. 8. In vitro ubiquitylation of HCV core protein by recombinant E6AP. For in vitro ubiquitylation of HCV core protein, purified GST-C173HT and GST-C152HT were used as substrates. Purified GST-HT was used as a negative control. Assays were done in 40-μl volumes containing each component as indicated. The reaction mixture is described in Materials and Methods. The reaction was carried out at 37°C for 120 min followed by purification with glutathione-Sepharose beads and analysis by immunoblotting with the indicated antibodies. Arrows indicate GST-C173HT, GST-C152HT, and GST-HT, respectively. Ubiquitylated species of GST-core proteins are marked by brackets. IB, immunoblot.

dilution assays. Exogenous expression of E6AP reduced the supernatant infectivity titer, whereas inactive E6AP had no effect on its infectivity titer (Fig. 9D), suggesting that the E6AP-dependent ubiquitin proteasome pathway affects the production of HCV particles through downregulation of the core protein.

E6AP silencing increases the levels of intracellular HCV core protein and supernatant infectivity titers in HCV-infected Huh-7 cells. Finally, to further validate the role of E6AP in HCV production, expression of endogenous E6AP was knocked down by siRNA and the HCV infectivity titers released from HCV JFH1-infected cells were examined. Knockdown of E6AP by siRNA led to an increase in intracellular core protein levels (Fig. 10A) and supernatant HCV infectivity titers (Fig. 10B). Taken together, our results suggest that E6AP mediates ubiquitylation and degradation of HCV core protein in HCV-infected cells, thereby affecting the production of HCV particles.

DISCUSSION

HCV core protein is a major component of viral nucleocapsid, plays a central role in viral assembly (25, 40), and contributes to viral pathogenesis and hepatocarcinogenesis (9). Therefore, it is important to clarify the molecular mechanisms that govern the cellular stability of this viral protein. We have previously reported that processing at the C-terminal hydrophobic domain of the core protein leads to efficient polyubiquitylation of the core protein (52). In this study, we identified E6AP as an HCV core-binding protein and showed that HCV core protein interacts with E6AP in vivo and in vitro, that E6AP enhances ubiquitylation and degradation of the mature core protein as well as the C-terminally truncated core protein, and that HCV core protein expressed from infectious HCV is degraded via E6AP-dependent proteolysis. HCV core protein and E6AP were found to colocalize in the cytoplasm, especially in the perinuclear region. Moreover, exogenous expression of E6AP reduces intracellular core protein levels and supernatant HCV infectivity titers in HCV-infected Huh-7 cells. Knockdown of endogenous E6AP by siRNA increases intracellular core protein levels and supernatant infectivity titers in HCV-infected cells. These findings suggest that E6AP mediates ubiquitylation and degradation of HCV core protein, thereby affecting the production of HCV particles.

HCV core protein interacts with E6AP through the region of the core protein between aa 58 and aa 71. These 14 amino acids are highly conserved, with the first nine amino acids (PRGRRQPIP) present in the core protein of all the HCV genotypes (3). This result suggests that E6AP-dependent degradation of HCV core protein is common to all HCV genotypes and plays an important role in the HCV life cycle or viral pathogenesis. Our data indicated that HCV core proteins of genotypes 1b and 2a are subjected to proteolysis through an E6AP-mediated degradation pathway. We are currently examining whether E6AP promotes degradation of HCV core proteins of other genotypes.

Studies in addition to ours have reported that other HCV proteins, such as NS5B (8), the unglycosylated cytosolic form of E2 (39), NS2 (7), and F protein (58), are degraded through the ubiquitin-proteasome pathway. These studies suggest that the ubiquitin-proteasome pathway plays a role in the HCV life cycle or viral pathogenesis. To our knowledge, the present study is the first to demonstrate that the ubiquitin-proteasome pathway affects the HCV life cycle.

PA28γ was found to interact with HCV core protein in hepatocytes and promote proteasomal degradation of HCV core protein (30). PA28γ, however, has been shown to function

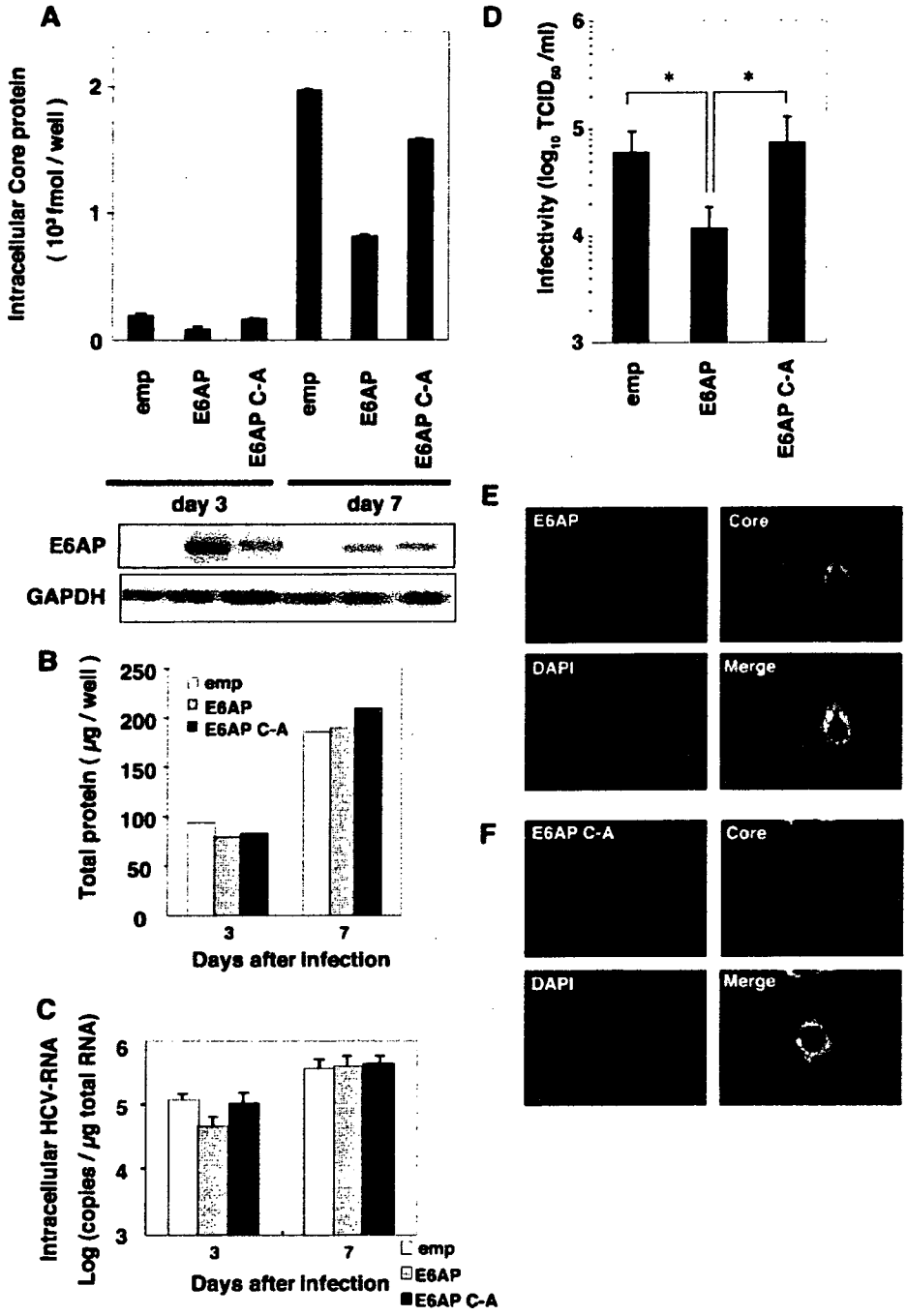

FIG. 9. Exogenous expression of E6AP reduces intracellular HCV core protein levels and supernatant infectivity titers in HCV-infected Huh-7 cells. Naïve Huh-7 cells were seeded as described in Materials and Methods; inoculated with 2.5 ml of the inoculum including infectious HCV JFH1 (6.5×10^3 $TCID_{50}$/ml); and transfected with 6 μg of empty plasmid, pCAG-HA-E6AP, or pCAG-HA-E6AP C-A. The culture supernatant and the cells were collected at days 3 and 7 postinfection. (A) Intracellular HCV core protein levels. (B) Levels of total protein. (C) Levels of intracellular HCV RNA in HCV-infected Huh-7 cells. Data represent the averages of three experiments with error bars. (D) Supernatant infectivity titers. At day 7 postinfection, culture supernatants were collected and assayed for $TCID_{50}$ determinations. The difference between empty vector and E6AP or between E6AP and E6AP C-A was significant (*, $P < 0.05$, Student's t test). (E and F) HCV JFH1-infected Huh-7 cells were transfected with either MEF-E6AP plasmid or MEF-E6AP C-A plasmid, grown on coverslips, fixed, and processed for double-label immunofluorescence for HCV core and MEF-E6AP (E) or MEF-E6AP C-A (F). Anticore MAb (2H9) and anti-FLAG PAb were used as primary antibodies. Nuclei were visualized by staining the cells with DAPI. All the samples were examined with a BZ-8000 microscope. Representative images of individual cells are shown with merge images. emp, empty vector.

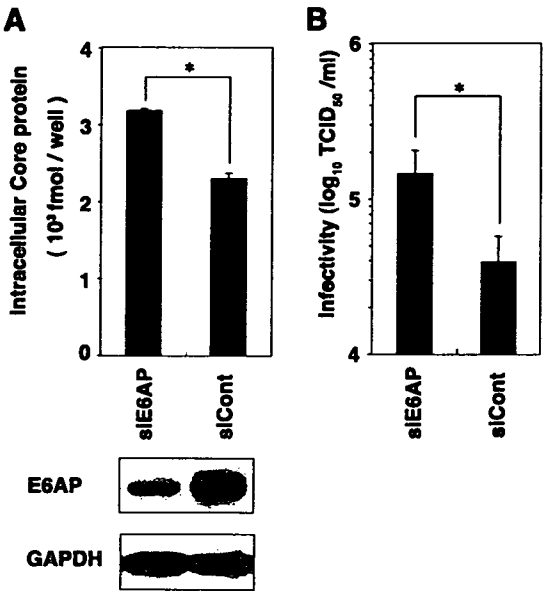

FIG. 10. E6AP silencing leads to an increase in the level of intracellular HCV core protein and supernatant infectivity titer in HCV-infected Huh-7 cells. (A) HCV JFH1-infected cells were replated in a six-well plate at 3×10^5 cells/well and transfected with 40 pmol of E6AP siRNA or control siRNA. The culture medium was changed at 24 h after transfection. The cells were harvested at day 2 after transfection, and the intracellular core protein levels were quantitated using the HCV core antigen ELISA. Equivalent amounts of the whole-cell lysates were separated by SDS-PAGE and analyzed by immunoblotting with anti-E6AP MAb or anti-GAPDH MAb. (B) Culture supernatants were collected at day 2 after transfection and assayed for $TCID_{50}$ determinations. For both panels, the difference between E6AP siRNA and control siRNA was significant (*, $P < 0.05$, Student's t test).

in a ubiquitin-independent, ATP-independent, and 20S proteasome-dependent pathway (27). There have been reports that several cellular factors, such as p53 (2), p73 (2), and RPN4 (18), are degraded through two alternative pathways, the ubiquitin-dependent 26S proteasome-dependent pathway and the ubiquitin-independent 20S proteasome-dependent pathway. Here we provide evidence that E6AP mediates ubiquitylation of HCV core protein. Still unclear is whether the PA28γ-dependent pathway requires polyubiquitylation of HCV core protein. HCV core protein is predominantly localized in the cytoplasm, especially at the endoplasmic reticulum membrane, on the surface of lipid droplets, and on mitochondria and mitochondrion-associated membranes (51). In HCV JFH1-infected cells, HCV core was found to localize in the cytoplasm and frequently to accumulate in the perinuclear region and the lipid droplets (44). Our results indicated that E6AP colocalized with HCV core protein especially in the perinuclear region. PA28γ was found to colocalize with HCV core protein in the nucleus. Functional differences may exist between the E6AP-dependent pathway and the PA28γ-dependent pathway in the stability control of HCV core protein. The functional role of the E6AP-dependent pathway and the PA28γ-dependent pathway remains to be elucidated.

The HCV core-binding region of E6AP was mapped to the region between aa 418 and aa 517. The multicopy maintenance protein 7, Mcm7, interacts with E6AP through a short motif, termed the L2G box (aa 412 to 414), that lies within the E6 binding site of E6AP (23). Our data indicated that the E6 binding region containing the L2G motif is not required for interaction between HCV core protein and E6AP (Fig. 2C, lane M).

We propose here that E6AP may affect the production of HCV particles through controlling the amounts of HCV core protein. This mechanism may contribute to persistent infection. The E6AP binding domain of the core protein resides in the RNA-binding domain and binding domains for many host factors (40). These factors may affect the binding between E6AP and HCV core protein, resulting in control of E6AP-dependent core degradation. Another possibility is that HCV core protein may affect the normal function of E6AP, thereby contributing to pathogenesis. It will be intriguing to investigate whether HCV core protein has any effect on E6AP-dependent degradation of host factors. The other intriguing possibility is that HCV core-E6AP complex may function as an E3 ligase-like E6-E6AP complex to target host factors for proteasomal degradation and contribute to viral pathogenesis.

In conclusion, we have demonstrated that E6AP interacts with HCV core protein in vitro and in vivo and mediates ubiquitin-dependent degradation of the core protein, leading to downregulation of HCV particles. We propose that the E6AP-mediated ubiquitin-proteasome pathway may play a role in affecting the production of HCV particles through controlling the amounts of viral nucleocapsid protein. Identification of the specific E3 ubiquitin ligase may contribute to gaining a better understanding of the biology of the HCV life cycle as well as molecular details of the ubiquitin-dependent degradation of HCV core protein.

ACKNOWLEDGMENTS

We thank D. Bohmann (EMBL) for providing pMT123, K. Miyazono (University of Tokyo) for pcDEF3-6Myc-WWP1, and K. Iwai (Osaka City University) for recombinant baculovirus carrying His 6-mouse E1. Huh-7.5.1 cells and Huh-7 cells were kindly provided by F. V. Chisari (Scripps Research Institute). We also thank P. Zhou (Weill Medical College of Cornell University), S. I. Wells (Cincinnati Children's Hospital Medical Center), and A. W. Hudson (Medical College of Wisconsin) for critical readings of the manuscript; M. Matsuda, S. Yoshizaki, M. Ikeda, and M. Sasaki for technical assistance; Y. Sugiyama and S. Senzui for plasmid construction; and T. Mizoguchi for secretarial work.

This work was supported in part by a grant for Research on Health Sciences focusing on Drug Innovation from the Japan Health Sciences Foundation; by grants-in-aid from the Ministry of Health, Labor and Welfare; by grants-in-aid from the Ministry of Education, Culture, Sports, Science and Technology; and by the program for Promotion of Fundamental Studies in Health Sciences of the National Institute of Biomedical Innovation (NIBIO), Japan. T.I. was supported in part by a grant from Novartis Foundation (Japan) for the Promotion of Science and by the Tokyo Metropolitan University President's Fund, Special Emphasis Research Project of Japan.

REFERENCES

1. **Aizaki, H., Y. Aoki, T. Harada, K. Ishii, T. Suzuki, S. Nagamori, G. Toda, Y. Matsuura, and T. Miyamura.** 1998. Full-length complementary DNA of hepatitis C virus genome from an infectious blood sample. Hepatology 27: 621–627.
2. **Asher, G., P. Tsvetkov, C. Kahana, and Y. Shaul.** 2005. A mechanism of ubiquitin-independent proteasomal degradation of the tumor suppressors p53 and p73. Genes Dev. 19:316–321.
3. **Bukh, J., R. H. Purcell, and R. H. Miller.** 1994. Sequence analysis of the core gene of 14 hepatitis C virus genotypes. Proc. Natl. Acad. Sci. USA 91:8239–8243.

4. **Chen, C., and H. Okayama.** 1987. High-efficiency transformation of mammalian cells by plasmid DNA. Mol. Cell. Biol. 7:2745–2752.
5. **Choo, Q. L., G. Kuo, A. J. Weiner, L. R. Overby, D. W. Bradley, and M. Houghton.** 1989. Isolation of a cDNA clone derived from a blood-borne non-A, non-B viral hepatitis genome. Science 244:359–362.
6. **Choo, Q. L., K. H. Richman, J. H. Han, K. Berger, C. Lee, C. Dong, C. Gallegos, D. Coit, R. Medina-Selby, P. J. Barr, et al.** 1991. Genetic organization and diversity of the hepatitis C virus. Proc. Natl. Acad. Sci. USA 88:2451–2455.
7. **Franck, N., J. Le Seyec, C. Guguen-Guillouzo, and L. Erdtmann.** 2005. Hepatitis C virus NS2 protein is phosphorylated by the protein kinase CK2 and targeted for degradation to the proteasome. J. Virol. 79:2700–2708.
8. **Gao, L., H. Tu, S. T. Shi, K. J. Lee, M. Asanaka, S. B. Hwang, and M. M. Lai.** 2003. Interaction with a ubiquitin-like protein enhances the ubiquitination and degradation of hepatitis C virus RNA-dependent RNA polymerase. J. Virol. 77:4149–4159.
9. **Giannini, C., and C. Brechot.** 2003. Hepatitis C virus biology. Cell Death Differ. 10(Suppl. 1):S27–S38.
10. **Grakoui, A., D. W. McCourt, C. Wychowski, S. M. Feinstone, and C. M. Rice.** 1993. Characterization of the hepatitis C virus-encoded serine proteinase: determination of proteinase-dependent polyprotein cleavage sites. J. Virol. 67:2832–2843.
11. **Harris, K. F., I. Shoji, E. M. Cooper, S. Kumar, H. Oda, and P. M. Howley.** 1999. Ubiquitin-mediated degradation of active Src tyrosine kinase. Proc. Natl. Acad. Sci. USA 96:13738–13743.
12. **Hijikata, M., H. Mizushima, T. Akagi, S. Mori, N. Kakiuchi, N. Kato, T. Tanaka, K. Kimura, and K. Shimotohno.** 1993. Two distinct proteinase activities required for the processing of a putative nonstructural precursor protein of hepatitis C virus. J. Virol. 67:4665–4675.
13. **Huibregtse, J. M., M. Scheffner, S. Beaudenon, and P. M. Howley.** 1995. A family of proteins structurally and functionally related to the E6-AP ubiquitin-protein ligase. Proc. Natl. Acad. Sci. USA 92:2563–2567.
14. **Huibregtse, J. M., M. Scheffner, and P. M. Howley.** 1993. Cloning and expression of the cDNA for E6-AP, a protein that mediates the interaction of the human papillomavirus E6 oncoprotein with p53. Mol. Cell. Biol. 13:775–784.
15. **Hussy, P., H. Langen, J. Mous, and H. Jacobsen.** 1996. Hepatitis C virus core protein: carboxy-terminal boundaries of two processed species suggest cleavage by a signal peptide peptidase. Virology 224:93–104.
16. **Ichimura, T., H. Yamamura, K. Sasamoto, Y. Tominaga, M. Taoka, K. Kakiuchi, T. Shinkawa, N. Takahashi, S. Shimada, and T. Isobe.** 2005. 14-3-3 proteins modulate the expression of epithelial Na^+ channels by phosphorylation-dependent interaction with Nedd4-2 ubiquitin ligase. J. Biol. Chem. 280:13187–13194.
17. **Iwai, K., K. Yamanaka, T. Kamura, N. Minato, R. C. Conaway, J. W. Conaway, R. D. Klausner, and A. Pause.** 1999. Identification of the von Hippel-Lindau tumor-suppressor protein as part of an active E3 ubiquitin ligase complex. Proc. Natl. Acad. Sci. USA 96:12436–12441.
18. **Ju, D., and Y. Xie.** 2004. Proteasomal degradation of RPN4 via two distinct mechanisms, ubiquitin-dependent and -independent. J. Biol. Chem. 279: 23851–23854.
19. **Kao, W. H., S. L. Beaudenon, A. L. Talis, J. M. Huibregtse, and P. M. Howley.** 2000. Human papillomavirus type 16 E6 induces self-ubiquitination of the E6AP ubiquitin-protein ligase. J. Virol. 74:6408–6417.
20. **Kato, T., M. Miyamoto, A. Furusaka, T. Date, K. Yasui, J. Kato, S. Matsushima, T. Komatsu, and T. Wakita.** 2003. Processing of hepatitis C virus core protein is regulated by its C-terminal sequence. J. Med. Virol. 69:357–366.
21. **Kishino, T., M. Lalande, and J. Wagstaff.** 1997. UBE3A/E6-AP mutations cause Angelman syndrome. Nat. Genet. 15:70–73.
22. **Komuro, A., T. Imamura, M. Saitoh, Y. Yoshida, T. Yamori, K. Miyazono, and K. Miyazawa.** 2004. Negative regulation of transforming growth factor-beta (TGF-beta) signaling by WW domain-containing protein 1 (WWP1). Oncogene 23:6914–6923.
23. **Kuhne, C., and L. Banks.** 1998. E3-ubiquitin ligase/E6-AP links multicopy maintenance protein 7 to the ubiquitination pathway by a novel motif, the L2G box. J. Biol. Chem. 273:34302–34309.
24. **Kumar, S., A. L. Talis, and P. M. Howley.** 1999. Identification of HHR23A as a substrate for E6-associated protein-mediated ubiquitination. J. Biol. Chem. 274:18785–18792.
25. **Kunkel, M., M. Lorinczi, R. Rijnbrand, S. M. Lemon, and S. J. Watowich.** 2001. Self-assembly of nucleocapsid-like particles from recombinant hepatitis C virus core protein. J. Virol. 75:2119–2129.
26. **Kuo, G., Q. L. Choo, H. J. Alter, G. L. Gitnick, A. G. Redeker, R. H. Purcell, T. Miyamura, J. L. Dienstag, M. J. Alter, C. E. Stevens, et al.** 1989. An assay for circulating antibodies to a major etiologic virus of human non-A, non-B hepatitis. Science 244:362–364.
27. **Li, X., D. M. Lonard, S. Y. Jung, A. Malovannaya, Q. Feng, J. Qin, S. Y. Tsai, M. J. Tsai, and B. W. O'Malley.** 2006. The SRC-3/AIB1 coactivator is degraded in a ubiquitin- and ATP-independent manner by the REGγ proteasome. Cell 124:381–392.
28. **Lindenbach, B. D., M. J. Evans, A. J. Syder, B. Wolk, T. L. Tellinghuisen, C. C. Liu, T. Maruyama, R. O. Hynes, D. R. Burton, J. A. McKeating, and C. M. Rice.** 2005. Complete replication of hepatitis C virus in cell culture. Science 309:623–626.
29. **McLauchlan, J., M. K. Lemberg, G. Hope, and B. Martoglio.** 2002. Intramembrane proteolysis promotes trafficking of hepatitis C virus core protein to lipid droplets. EMBO J. 21:3980–3988.
30. **Moriishi, K., T. Okabayashi, K. Nakai, K. Moriya, K. Koike, S. Murata, T. Chiba, K. Tanaka, R. Suzuki, T. Suzuki, T. Miyamura, and Y. Matsuura.** 2003. Proteasome activator PA28γ-dependent nuclear retention and degradation of hepatitis C virus core protein. J. Virol. 77:10237–10249.
31. **Moriya, K., H. Fujie, Y. Shintani, H. Yotsuyanagi, T. Tsutsumi, K. Ishibashi, Y. Matsuura, S. Kimura, T. Miyamura, and K. Koike.** 1998. The core protein of hepatitis C virus induces hepatocellular carcinoma in transgenic mice. Nat. Med. 4:1065–1067.
32. **Moriya, K., H. Yotsuyanagi, Y. Shintani, H. Fujie, K. Ishibashi, Y. Matsuura, T. Miyamura, and K. Koike.** 1997. Hepatitis C virus core protein induces hepatic steatosis in transgenic mice. J. Gen. Virol. 78:1527–1531.
33. **Natsume, T., Y. Yamauchi, H. Nakayama, T. Shinkawa, M. Yanagida, N. Takahashi, and T. Isobe.** 2002. A direct nanoflow liquid chromatography-tandem mass spectrometry system for interaction proteomics. Anal. Chem. 74:4725–4733.
34. **Niwa, H., K. Yamamura, and J. Miyazaki.** 1991. Efficient selection for high-expression transfectants with a novel eukaryotic vector. Gene 108:193–199.
35. **Oda, H., S. Kumar, and P. M. Howley.** 1999. Regulation of the Src family tyrosine kinase Blk through E6AP-mediated ubiquitination. Proc. Natl. Acad. Sci. USA 96:9557–9562.
36. **Ogino, T., H. Fukuda, S. Imajoh-Ohmi, M. Kohara, and A. Nomoto.** 2004. Membrane binding properties and terminal residues of the mature hepatitis C virus capsid protein in insect cells. J. Virol. 78:11766–11777.
37. **Okamoto, K., K. Moriishi, T. Miyamura, and Y. Matsuura.** 2004. Intramembrane proteolysis and endoplasmic reticulum retention of hepatitis C virus core protein. J. Virol. 78:6370–6380.
38. **Owsianka, A. M., and A. H. Patel.** 1999. Hepatitis C virus core protein interacts with a human DEAD box protein DDX3. Virology 257:330–340.
39. **Pavio, N., D. R. Taylor, and M. M. Lai.** 2002. Detection of a novel unglycosylated form of hepatitis C virus E2 envelope protein that is located in the cytosol and interacts with PKR. J. Virol. 76:1265–1272.
40. **Polyak, S. J., K. C. Klein, I. Shoji, T. Miyamura, and J. R. Lingappa.** 2006. Assemble and interact: pleiotropic functions of the HCV core protein, p. 89–119. *In* S.-L. Tan (ed.), Hepatitis C viruses: genomes and molecular biology. Horizon Bioscience, Norwich, United Kingdom.
41. **Poynard, T., M. F. Yuen, V. Ratziu, and C. L. Lai.** 2003. Viral hepatitis C. Lancet 362:2095–2100.
42. **Ravaggi, A., G. Natoli, D. Primi, A. Albertini, M. Levrero, and E. Cariani.** 1994. Intracellular localization of full-length and truncated hepatitis C virus core protein expressed in mammalian cells. J. Hepatol. 20:833–836.
43. **Ray, R. B., L. M. Lagging, K. Meyer, and R. Ray.** 1996. Hepatitis C virus core protein cooperates with *ras* and transforms primary rat embryo fibroblasts to tumorigenic phenotype. J. Virol. 70:4438–4443.
44. **Rouille, Y., F. Helle, D. Delgrange, P. Roingeard, C. Voisset, E. Blanchard, S. Belouzard, J. McKeating, A. H. Patel, G. Maertens, T. Wakita, C. Wychowski, and J. Dubuisson.** 2006. Subcellular localization of hepatitis C virus structural proteins in a cell culture system that efficiently replicates the virus. J. Virol. 80:2832–2841.
45. **Saito, I., T. Miyamura, A. Ohbayashi, H. Harada, T. Katayama, S. Kikuchi, Y. Watanabe, S. Koi, M. Onji, Y. Ohta, et al.** 1990. Hepatitis C virus infection is associated with the development of hepatocellular carcinoma. Proc. Natl. Acad. Sci. USA 87:6547–6549.
46. **Santolini, E., G. Migliaccio, and N. La Monica.** 1994. Biosynthesis and biochemical properties of the hepatitis C virus core protein. J. Virol. 68: 3631–3641.
47. **Sato, S., M. Fukasawa, Y. Yamakawa, T. Natsume, T. Suzuki, I. Shoji, H. Aizaki, T. Miyamura, and M. Nishijima.** 2006. Proteomic profiling of lipid droplet proteins in hepatoma cell lines expressing hepatitis C virus core protein. J. Biochem. (Tokyo) 139:921–930.
48. **Scheffner, M., J. M. Huibregtse, and P. M. Howley.** 1994. Identification of a human ubiquitin-conjugating enzyme that mediates the E6-AP-dependent ubiquitination of p53. Proc. Natl. Acad. Sci. USA 91:8797–8801.
49. **Scheffner, M., J. M. Huibregtse, R. D. Vierstra, and P. M. Howley.** 1993. The HPV-16 E6 and E6-AP complex functions as a ubiquitin-protein ligase in the ubiquitination of p53. Cell 75:495–505.
50. **Scheffner, M., U. Nuber, and J. M. Huibregtse.** 1995. Protein ubiquitination involving an E1–E2–E3 enzyme ubiquitin thioester cascade. Nature 373:81–83.
51. **Suzuki, R., S. Sakamoto, T. Tsutsumi, A. Rikimaru, K. Tanaka, T. Shimoike, K. Moriishi, T. Iwasaki, K. Mizumoto, Y. Matsuura, T. Miyamura, and T. Suzuki.** 2005. Molecular determinants for subcellular localization of hepatitis C virus core protein. J. Virol. 79:1271–1281.
52. **Suzuki, R., K. Tamura, J. Li, K. Ishii, Y. Matsuura, T. Miyamura, and T. Suzuki.** 2001. Ubiquitin-mediated degradation of hepatitis C virus core pro-

tein is regulated by processing at its carboxyl terminus. Virology 280:301–309.
53. Suzuki, T., K. Omata, T. Satoh, T. Miyasaka, C. Arai, M. Maeda, T. Matsuno, and T. Miyamura. 2005. Quantitative detection of hepatitis C virus (HCV) RNA in saliva and gingival crevicular fluid of HCV-infected patients. J. Clin. Microbiol. 43:4413–4417.
54. Takamizawa, A., C. Mori, I. Fuke, S. Manabe, S. Murakami, J. Fujita, E. Onishi, T. Andoh, I. Yoshida, and H. Okayama. 1991. Structure and organization of the hepatitis C virus genome isolated from human carriers. J. Virol. 65:1105–1113.
55. Talis, A. L., J. M. Huibregtse, and P. M. Howley. 1998. The role of E6AP in the regulation of p53 protein levels in human papillomavirus (HPV)-positive and HPV-negative cells. J. Biol. Chem. 273:6439–6445.
56. Wakita, T., T. Pietschmann, T. Kato, T. Date, M. Miyamoto, Z. Zhao, K. Murthy, A. Habermann, H. G. Krausslich, M. Mizokami, R. Bartenschlager, and T. J. Liang. 2005. Production of infectious hepatitis C virus in tissue culture from a cloned viral genome. Nat. Med. 11:791–796.
57. Wertz, I. E., K. M. O'Rourke, Z. Zhang, D. Dornan, D. Arnott, R. J. Deshaies, and V. M. Dixit. 2004. Human de-etiolated-1 regulates c-Jun by assembling a CUL4A ubiquitin ligase. Science 303:1371–1374.
58. Xu, Z., J. Choi, W. Lu, and J. Ou. 2003. Hepatitis C virus F protein is a short-lived protein associated with the endoplasmic reticulum. J. Virol. 77:1578–1583.
59. Yamaguchi, R., S. Momosaki, G. Gao, C. C. Hsia, M. Kojiro, C. Scudamore, and E. Tabor. 2004. Truncated hepatitis C virus core protein encoded in hepatocellular carcinomas. Int. J. Mol. Med. 14:1097–1100.
60. Yasui, K., T. Wakita, K. Tsukiyama-Kohara, S. I. Funahashi, M. Ichikawa, T. Kajita, D. Moradpour, J. R. Wands, and M. Kohara. 1998. The native form and maturation process of hepatitis C virus core protein. J. Virol. 72:6048–6055.
61. Zhong, J., P. Gastaminza, G. Cheng, S. Kapadia, T. Kato, D. R. Burton, S. F. Wieland, S. L. Uprichard, T. Wakita, and F. V. Chisari. 2005. Robust hepatitis C virus infection in vitro. Proc. Natl. Acad. Sci. USA 102:9294–9299.

Arch Virol (2007) 152: 457–461
DOI 10.1007/s00705-006-0883-z
Printed in The Netherlands

Archives of Virology

Brief Review

Binding activity of norovirus and sapovirus to histo-blood group antigens

H. Shirato-Horikoshi, S. Ogawa, T. Wakita, N. Takeda, and **G. S. Hansman**

Department of Virology II, National Institute of Infectious Diseases, Tokyo, Japan

Received August 22, 2006; accepted October 26, 2006; published online November 27, 2006

Summary

Noroviruses (NoVs) and sapoviruses (SaVs) are causative agents of human gastroenteritis. There is increasing evidence that certain human NoV strains bind to histo-blood group antigens (HBGAs). We found that several NoV virus-like particles (VLPs) showed binding activity to HBGAs, while neither SaV genogroup I (GI) VLP nor SaV GV VLP showed such activity.

*

Human noroviruses (NoVs) and human sapoviruses (SaVs) are etiological agents of human gastroenteritis. Human NoV strains can be grouped into two genogroups (GI and GII), and at least 14 GI and 17 GII genotypes (GI/1–14 and GII/1–17) [11]. SaV strains can be divided into five genogroups (GI–GV), of which the GI, GII, GIV and GV strains infect humans, while the GIII strains infect porcine species [1]. Human NoV and SaV strains are noncultivable, but the expression of the recombinant capsid protein VP1 (rVP1) in insect cells results in the self-assembly of virus-like particles (VLPs) that are antigenically similar to native viruses [2, 9]. In the past several years, increasing evidence has emerged that human NoVs bind to histo-blood group antigens (HBGAs) [8, 12]. These carbohydrate epitopes are present in mucosal secretions and throughout many tissues of the human body, including the small intestine, which may be specifically targeted by certain NoV strains. To the best of our knowledge, the relationship between human SaVs and HBGAs has not yet been reported.

In the present study, we examined the binding activities of human NoV and SaV VLPs to HBGAs present in human saliva and to synthetic carbohydrates. Four NoV strains belonging to different genotypes were examined: the GI/1 124 strain (accession number AB031013), the GI/2 258 strain (AB078335), the GII/4 104 strain (AB078336), and the GII/1 Hawaii strain (U07611). Hawaii VLPs were used as a negative control [5]. Two SaV strains belonging to two different genogroups were also examined: the SaV GI Mc114 strain (AY237422) and the SaV GV NK24 strain (AY646856). Saliva samples were collected from 29 healthy donors. The amounts of Lewis a (Le^a), Lewis b (Le^b), H, A and B antigens in the saliva samples were determined semi-quantitatively by hemagglutination inhibition, and 12 saliva samples with relatively high amounts

Author's address: Dr. Grant Hansman, Department of Virology II, National Institute of Infectious Diseases, Gakuen 4-7-1, Musashi-murayama, Tokyo 208-0011, Japan.
e-mail: ghansman@nih.go.jp

Table 1. Semiquantitation of soluble ABH and Lewis antigens

Donor no.	Interpretation of saliva testing	Grouping	Hemagglutination inhibition titer				
			H	A	B	Lewis-a	Lewis-b
1	Secretor/O/Lewis-positive	H^{high}/Le-b^{high}	>256	0	0	32	32
2	Secretor/O/Lewis-positive		>256	0	0	32	32
3	Secretor/O/Lewis-positive		128	0	0	32	64
4	Secretor/AB/Lewis-positive	A^{high}	16	>256	32	8	2
5	Secretor/AB/Lewis-positive		8	>256	8	8	4
6	Secretor/AB/Lewis-positive		16	128	8	4	4
7	Secretor/B/Lewis-negative	B^{high}	16	0	>256	0	0
8	Secretor/B/Lewis-positive		16	0	128	16	4
9	Secretor/B/Lewis-positive		16	0	128	2	4
10	Nonsecretor	Le-a^{high}	4	8	0	>256	8
11	Nonsecretor		4	1	0	>256	4
12	Nonsecretor		0	1	0	>256	4

of antigens were selected for saliva-VLP binding assay (Table 1). We then used 2 enzyme-linked immunosorbent assay (ELISA)-based assays, a saliva-VLP binding assay and a carbohydrate-VLP binding assay to examine the binding activities of the NoV and SaV VLPs to HBGAs.

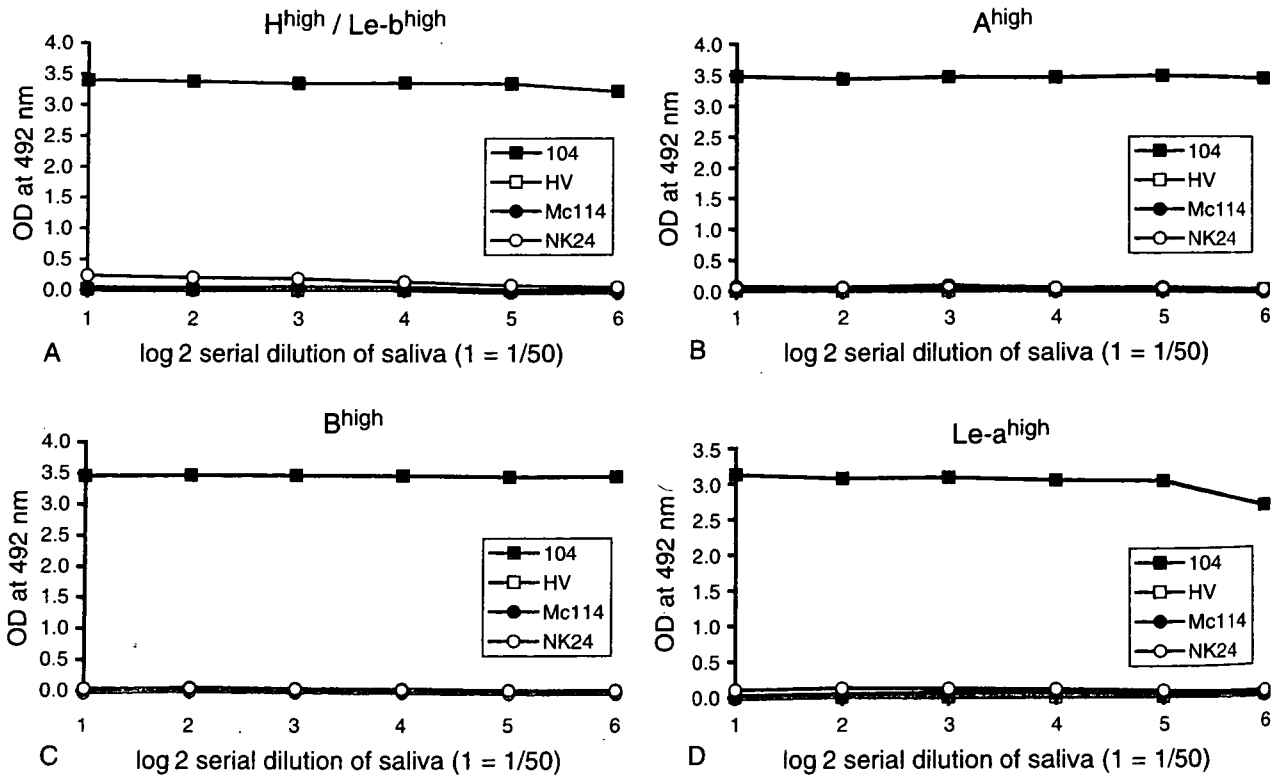

Fig. 1. NoV and SaV VLP binding activity to the saliva samples. Optical densities were measured at 492 nm and were plotted against the serial diluted saliva samples. Each experiment was performed with three donors from each HBGA group (Table 1) and repeated twice. Three samples from the same group produced similar results (data not shown). The results from the donors 1 (**A**), 4 (**B**), 7 (**C**) and 10 (**D**) are shown

In the saliva-VLP binding assay, we examined the possibility that NoV and SaV VLPs may bind to saliva samples. Briefly, 100 µl of serially diluted saliva samples dissolved in carbonate/bicarbonate buffer (50 mmol/L, pH 9.6) were added to wells and incubated at 37 °C overnight. The wells were washed 3–6 times with 300 µl of phosphate-buffered saline containing 0.05% Tween 20 (PBS-T) and washed again after each of the following steps. The wells were blocked with 200 µl of PBS containing 5% skim milk (SM/PBS) for 1 h at room temperature. The purified VLPs, dissolved in 1% SM/PBS-T (final 1 µg/mL), were added (100 µl) to the wells and incubated for 1 h at 37 °C. Next, 100 µl of rabbit anti-rSaV or NoV VLP antiserum (1:2000) in 1% SM/PBS-T was added, and incubated for 1 h at 37 °C. Horseradish peroxidase (HRP)-conjugated anti-rabbit IgG (100 µl; Zymed Laboratories Inc., San Francisco, CA, USA) in 1% SM/PBS-T was then added and incubated for 1 h at 37 °C. One hundred microliter of O-phenylenediamine (Sigma, St. Louis, MO, USA) was added as substrate, and incubated at room temperature for 30 min, at which point 50 µl of 4N H_2SO_4 was added to stop the reaction, and the optical density (OD) at 492 nm was measured. The wells incubated with carbonate/bicarbonate buffer instead of serially diluted saliva samples were used as plate blank (Fig. 1). The Hawaii VLPs have been reported to show no binding to HBGAs [5]; under the present experimental conditions, Hawaii VLPs also showed no binding activity (OD values less than 0.01) at all to HBGAs in saliva. The VLPs of the NoV 104 strain, which resembles Camberwell virus (AF145896) and is classified into GII/4, showed strong binding activity to the diluted saliva at all dilutions of all HBGA samples (OD values greater than 2.7), while SaV Mc114 VLPs showed little binding activity at all dilutions of all samples (OD less than 0.09), as did SaV NK24 VLPs (OD values less than 0.24). These results indicate that the SaV Mc114 and NK24 VLPs have no binding activity with saliva antigens.

In the carbohydrate-VLP binding assay, we examined the possibility that NoV and SaV VLPs may bind to different synthetic carbohydrates, such as H-1 (trisaccharides), A (trisaccharides), B (trisaccharides), Le^a (trisaccharides) and Le^b (tetrasaccharides). Briefly, multivalent carbohydrate-biotin reagents conjugated to polyacrylamide (CHO-PAA-biotin; GlycoTech, Rockville, MD, USA) were resuspended in 0.3 M sodium phosphate buffer at 1 mg/ml, diluted to 20 µg/ml in Tris-buffered saline, and serially diluted twofold, after which 100 µl was added per well to streptavidin-precoated plates (Thermo Labsystems, Basingstoke, United Kingdom) and incubated for 2 h at 37 °C. The wells were washed 3–6 times with PBS-T and were washed again after each of the following steps. The plates were blocked with 300 µl of 5% SM/PBS overnight at 4 °C. The VLPs (1 µg/ml in 100 µl of 5% SM/PBS) were added to each well and incubated for 4 h at 37 °C. Next, 100 µl of rabbit anti-rNoV VLPs antiserum (1:2000 in 5% SM/PBS) was added and incubated for 2 h at 37 °C. One hundred microliter of HRP-conjugated anti-rabbit IgG in 5% SM/PBS was then added and incubated for 1 h at 37 °C. The plates were processed as described above. The wells incubated with Tris-buffered saline and 5% SM/PBS instead of serially diluted synthetic carbohydrates and VLPs were used as plate blank.

The NoV 104 VLPs were found to show strong binding activity to three of five synthetic carbohydrates: A, B and Le^b (Fig. 2B, C and E). Although 104 VLPs showed strong binding activity to the saliva samples containing relatively high amounts of H antigen (Fig. 1A) and Le^a antigen (Fig. 1D), they showed only moderate binding activity to H synthetic carbohydrates and no binding activity to Le^a synthetic carbohydrates (Fig. 2A and D). Differences in the reactivity between saliva samples and synthetic carbohydrates may be due to differences between synthetic products and the authentic antigens found in vivo, which are thought to be present on mucin or mucin-like molecules [7]. Therefore, we included two additional NoV VLPs, the 124 and 258 VLPs, as positive controls for the H and Le^a synthetic carbohydrates (Fig. 2A and D), respectively, which showed strong binding activity to the H-high and Le^a-high saliva samples (data not shown). The 124 strain is genetically close to the GI/1 prototype Norwalk virus (NV/68; M87661), and the binding properties of recombinant NV/68

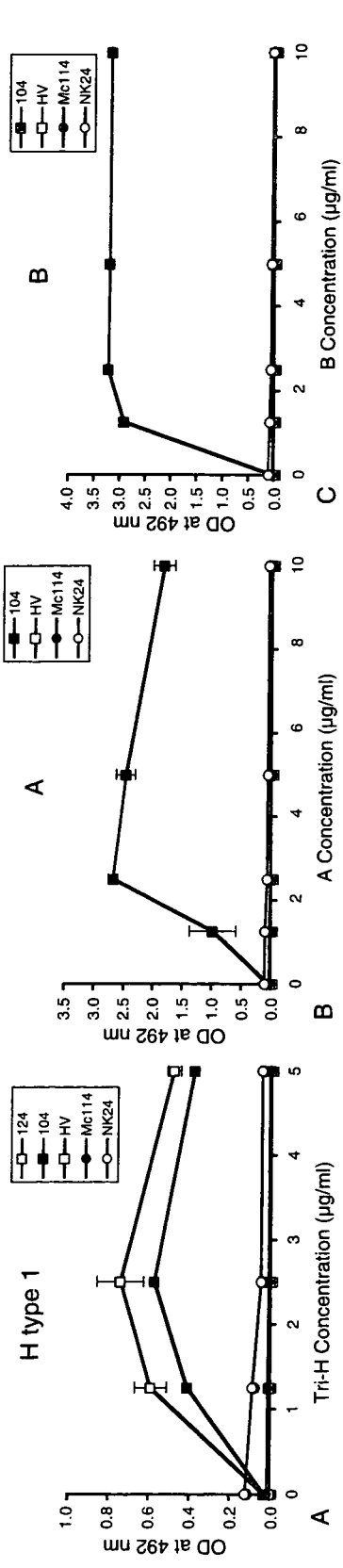

Fig. 2. NoV and SaV VLP binding activity to the synthetic carbohydrates. The optical densities at 492 nm are plotted against the dilutions. Each experiment was performed in duplicate and repeated twice

to H antigen have been well characterized [5, 13]. The 124 strain showed 99% amino acid identity with NV/68 in the P2 domain. There are known to be two amino acid differences at residues 370 and 376 which are not related to HBGA binding [14]. The 258 strain resembles Southampton virus (L07418) and is classified into GI/2. The NoV Hawaii VLPs showed no binding activity to any of these synthetic carbohydrates (Fig. 2). The SaV Mc114 and NK24 VLPs also showed no binding activity to any of the synthetic carbohydrates (Fig. 2).

A number studies have found that different NoV strains exhibit different binding patterns to HBGAs [5–7]. In the present study, we found that NoV GII/4 104 VLPs showed binding activity to HBGAs, while SaV GI and GV VLPs showed no such binding activity. Human SaVs are becoming an increasingly important cause of gastroenteritis worldwide [3, 4, 10]. Further studies are needed to examine the possibility that other human SaV genogroups have binding activity.

Acknowledgements

This work was supported in part by a grant for Research on Emerging and Re-emerging Infectious Diseases, Research on Food Safety from the Ministry of Health, Labor and Welfare of Japan, and by a grant for Research on Health Science Focusing on Drug Innovation from The Japan Health Science Foundation.

References

1. Farkas T, Zhong WM, Jing Y, Huang PW, Espinosa SM, Martinez N, Morrow AL, Ruiz-Palacios GM, Pickering LK, Jiang X (2004) Genetic diversity among sapoviruses. Arch Virol 149: 1309–1323
2. Hansman GS, Natori K, Oka T, Ogawa S, Tanaka K, Nagata N, Ushijima H, Takeda N, Katayama K (2005) Cross-reactivity among sapovirus recombinant capsid proteins. Arch Virol 150: 21–36
3. Hansman GS, Takeda N, Oka T, Oseto M, Hedlund KO, Katayama K (2005) Intergenogroup recombination in sapoviruses. Emerg Infect Dis 11: 1916–1920
4. Hansman GS, Takeda N, Katayama K, Tu ET, McIver CJ, Rawlinson WD, White PA (2006) Genetic diversity of Sapovirus in children, Australia. Emerg Infect Dis 12: 141–143
5. Harrington PR, Lindesmith L, Yount B, Moe CL, Baric RS (2002) Binding of Norwalk virus-like particles to ABH histo-blood group antigens is blocked by antisera from infected human volunteers or experimentally vaccinated mice. J Virol 76: 12335–12343
6. Huang P, Farkas T, Marionneau S, Zhong W, Ruvoen-Clouet N, Morrow AL, Altaye M, Pickering LK, Newburg DS, LePendu J, Jiang X (2003) Noroviruses bind to human ABO, Lewis, and secretor histo-blood group antigens: identification of 4 distinct strain-specific patterns. J Infect Dis 188: 19–31
7. Huang P, Farkas T, Zhong W, Tan M, Thornton S, Morrow AL, Jiang X (2005) Norovirus and histo-blood group antigens: demonstration of a wide spectrum of strain specificities and classification of two major binding groups among multiple binding patterns. J Virol 79: 6714–6722
8. Hutson AM, Atmar RL, Graham DY, Estes MK (2002) Norwalk virus infection and disease is associated with ABO histo-blood group type. J Infect Dis 185: 1335–1337
9. Jiang X, Wang M, Graham DY, Estes MK (1992) Expression, self-assembly, and antigenicity of the Norwalk virus capsid protein. J Virol 66: 6527–6532
10. Johansson PJ, Bergentoft K, Larsson PA, Magnusson G, Widell A, Thorhagen M, Hedlund KO (2005) A nosocomial sapovirus-associated outbreak of gastroenteritis in adults. Scand J Infect Dis 37: 200–204
11. Kageyama T, Shinohara M, Uchida K, Fukushi S, Hoshino FB, Kojima S, Takai R, Oka T, Takeda N, Katayama K (2004) Coexistence of multiple genotypes, including newly identified genotypes, in outbreaks of gastroenteritis due to Norovirus in Japan. J Clin Microbiol 42: 2988–2995
12. Lindesmith L, Moe C, Marionneau S, Ruvoen N, Jiang X, Lindblad L, Stewart P, LePendu J, Baric R (2003) Human susceptibility and resistance to Norwalk virus infection. Nat Med 9: 548–553
13. Marionneau S, Ruvoen N, Le Moullac-Vaidye B, Clement M, Cailleau-Thomas A, Ruiz-Palacois G, Huang P, Jiang X, Le Pendu J (2002) Norwalk virus binds to histo-blood group antigens present on gastroduodenal epithelial cells of secretor individuals. Gastroenterology 122: 1967–1977
14. Tan M, Huang P, Meller J, Zhong W, Farkas T, Jiang X (2003) Mutations within the P2 domain of norovirus capsid affect binding to human histo-blood group antigens: evidence for a binding pocket. J Virol 77: 12562–12571

PROTOCOL

Cell culture and infection system for hepatitis C virus

Takanobu Kato[1], Tomoko Date[2], Asako Murayama[2], Kenichi Morikawa[2], Daisuke Akazawa[2,3] & Takaji Wakita[2]

[1]Liver Diseases Branch, National Institute of Diabetes and Digestive and Kidney Diseases, National Institutes of Health, Bethesda, Maryland 20892, USA. [2]Department of Virology II, National Institute of Infectious Diseases, Shinjuku, Tokyo 162-8640, Japan. [3]Pharmaceutical Research Lab, Toray Industries, Kanagawa 248-8555, Japan. Correspondence should be addressed to T.W. (wakita@nih.go.jp).

Published online 21 December 2006; doi:10.1038/nprot.2006.395

Hepatitis C virus (HCV) infection causes chronic liver disease and is a worldwide health problem. Despite ever-increasing demand for knowledge on viral replication and pathogenesis, detailed analysis has been hampered by a lack of efficient viral culture systems. We isolated HCV genotype 2a strain JFH-1 from a patient with fulminant hepatitis. This strain replicates efficiently in Huh7 cells. Efficient replication and secretion of recombinant viral particles can be obtained in cell culture by transfection of *in vitro*–transcribed full-length JFH-1 RNA into Huh7 cells. JFH-1 virus generated in cell culture is infectious for both naive Huh7 cells and chimpanzees. The efficiency of viral production and infectivity of generated virus is substantially improved with permissive cell lines. This protocol describes how to use this system, which provides a powerful tool for studying viral life cycle and for the construction of antiviral strategies and the development of effective vaccines. Viral particles can be obtained in 12 days with this protocol.

INTRODUCTION

Hepatitis C virus (HCV) is a chief causative agent of chronic liver disease and affects about 170 million people worldwide at present. This virus has the ability to cause persistent infection in susceptible hosts after parenteral transmission, and the underlying mechanisms are not well understood. No vaccine protecting against HCV infection is available. Therapy for HCV-related chronic hepatitis remains problematic, with limited efficacy, high cost and substantial adverse effects. Understanding the biology of this virus and developing new therapies have been hampered by a lack of appropriate model systems for replication and infection. Although many attempts have been made to establish an *in vivo* model that mimics HCV replication, sufficient replication has not been achieved. A unique HCV genotype 2a strain, JFH-1, was isolated from a Japanese patient with fulminant hepatitis[1]. This strain was found to replicate efficiently in cultured cells as a subgenomic replicon in the Huh7 human hepatoma cell line[2]. Using this strain, an efficient cell culture and infection system for HCV has been established[3,4].

Isolation of the JFH-1 strain

The HCV JFH-1 strain was isolated from a patient with fulminant hepatitis[1]. The patient was a 32-year-old man who was admitted with general fatigue, high-grade fever and liver dysfunction. He had high concentrations of serum aspartate aminotransferase and alanine aminotransferase, a low minimum prothrombin time and stage II encephalopathy. HCV RNA was detected by RT-PCR, and the patient was negative for antibodies to HCV. All other hepatitis virus markers were negative. The patient was diagnosed with HCV-associated fulminant hepatitis. HCV RNA was isolated from acute-phase serum and the entire genome was sequenced. The genome of this HCV strain, designated JFH-1, was analyzed phylogenetically and was classified as genotype 2a, but a slight deviation from other genotype 2a strains was identified[1].

Replication and viral secretion of JFH-1 strain in cell culture

For investigation of the replication capacity of this JFH-1 strain, a subgenomic JFH-1 replicon was constructed[2]. Colony formation efficiency of JFH-1 replicon was much higher than that of the prototype Con1 replicon or the adaptive mutants containing Con1 replicon in Huh7 cells. This JFH-1 replicon replicated not only in Huh7 cells but also in the HepG2 and IMY-N9 hepatocyte-derived cell lines and the HeLa and 293 non-hepatocyte-derived cell lines[5,6]. That difference may be due to the replication capacity of JFH-1. Notably, the JFH-1 replicon did not require an adaptive mutation to replicate in those cell lines[2,5,6]. Full-length HCV RNA containing multiple cell-culture adaptive mutations has been reported as not demonstrating active HCV infection[7]. High replication capacity without the need for adaptive mutations thus seems to be an important factor in development of an HCV infection system.

Taking advantage of that replication efficiency, full-length JFH-1 cDNA was constructed for use in assaying replication of viral RNA in transfected Huh7 cells[3]. JFH-1 consensus full-length cDNA has been cloned from RT-PCR fragments. For production of full-length JFH-1 RNA, the T7 promoter sequence was inserted immediately upstream of the full-length JFH-1 cDNA sequence and then used T7 RNA polymerase to transcribe the RNA. When synthesized full-length JFH-1 RNA was transfected into naive Huh7 cells, viral RNA replication and viral protein expression were found in transfected cells. Secretion of viral particles into culture medium was confirmed by sucrose density gradient assay. Viral RNA and all structural proteins (core, E1 and E2) were detected in fractions with a density of around 1.15–1.17 g ml^{-1}, suggesting the formation and secretion of complete viral particles. Immuno-electron microscopy was used to visualize viral particles; a spherical form of about 55 nm diameter was demonstrated by Bartenschlager's group (University of Heidelberg, Heidelberg, Germany)[3]. The *in vitro* infectivity of the cell culture generated JFH-1 virus was monitored by inoculation of naive Huh7 cells with the culture medium of JFH-1 RNA–transfected cells. Infectivity could be detected by indirect immunofluorescence microscopy, although the infectious titer was very low. The *in vivo* infectivity of this cell culture generated virus was also assessed by inoculation of a chimpanzee by Liang's group (National Institutes of Health, Bethesda, Maryland)[3]. The chimpanzee established transient viremia after inoculation of culture medium containing 8×10^3 copies of HCV RNA. These experiments confirmed both the *in vitro* and *in vivo* infectivity of cell culture–generated JFH-1 virus.

Permissive cell lines for HCV replication

To our knowledge, JFH-1 is the first HCV strain found to replicate efficiently and produce infectious virus particles in cultured cells. However, the efficiency of virus generation and infection was very low in the first study with standard Huh7 cells. That limitation was overcome with permissive cell lines[4,8]. Those cells were generated from replicon cell lines by eradication of the replicon with interferon-α and interferon-γ, and they are known to support HCV replication in replicon studies[4,9]. Efficient production of infectious JFH-1 virus in Huh7.5.1 cells or infectious chimeric virus in Huh7.5 cells have been independently reported by Chisari's group (Scripps Research Institute, La Jolla, California)[4] and Rice's group (Rockefeller University, New York, New York)[8]. All the groups used a similar procedure to produce virus particles. They also found that Huh7.5 and Huh7.5.1 cells were more susceptible to virus infection than were the standard Huh7 cells. These cell lines are capable of contributing to efficient viral production and infection in this system.

Biohazardous materials

Classifications for levels of infectious agents differ among countries. Furthermore, regulations regarding infectious agents differ among institutes and countries. Infectious HCV should be handled according to the applicable regulations. For example, HCV is infectious for humans and is designated a 'level 2' infectious agents in Japan and the United States and 'level 3' in France. HCV should thus be handled in a Biosafety Level 2 or Level 3 facility according to national regulations[10]. All liquid and solid wastes should be disposed of after autoclaving.

MATERIALS

REAGENTS

- Plasmid for full-length JFH-1 RNA transcription (pJFH1) ▲ CRITICAL The entire sequence of pJFH1 should be confirmed before use.
- Restriction enzyme *XbaI* (high concentration) and reaction buffer (NEBuffer 2; New England BioLabs, cat. no. R0145M)
- Nuclease-free water (Ambion, cat. no. 9938)
- 1 Kb Plus DNA Ladder (Invitrogen, cat. no. 10787-018)
- Ethidium bromide (10 mg ml^{-1}; Invitrogen, cat. no. 15585-011) ! CAUTION Ethidium bromide is mutagenic. Wear gloves when handling.
- Phenol–chloroform–isoamyl alcohol (25:24:1 (vol/vol/vol); Invitrogen, cat. no. 15593-031) ! CAUTION The phenol–chloroform–isoamyl alcohol mixture is harmful. Handle with appropriate safety equipment.
- Chloroform (Sigma, cat. no. C2432) ! CAUTION Chloroform is harmful. Handle with appropriate safety equipment.
- 3 M sodium acetate
- Ethanol (molecular biology grade), 99.5% and 70%
- Glycogen (molecular biology grade)
- Mung bean nuclease and buffer (New England BioLabs, cat. no. M0250S)
- Proteinase K (Invitrogen, cat. no. 25530-049)
- SDS (Sigma, cat. no. L4390) ! CAUTION SDS is harmful. Handle with appropriate safety equipment.
- λ DNA–*Hin*dIII fragment marker (Invitrogen, cat. no. 15612-013)
- MEGAscript T7 kit (Ambion, cat. no. 1334)
- TRIzol LS (Invitrogen, cat. no. 10296-010) ! CAUTION This reagent contains phenol and is harmful. Handle with appropriate safety equipment.
- RNA ladder (New England BioLabs, cat. no. N0362S)
- Huh7 cells
- Trypsin-EDTA (liquid; Invitrogen, cat. no. 25300-054)
- OptiMEM I reduced-serum medium (Invitrogen, cat. no. 31985-070)
- Cytomix buffer[11] (see REAGENT SETUP)
- Adenosine 5′-triphosphate (ATP; Sigma, cat. no. A-7699)
- L-glutathione (Sigma, cat. no. G-6529)
- Complete medium (see REAGENT SETUP)
- DMEM (low-glucose; Invitrogen, cat. no. 12567-014)
- FBS (appropriate lot for Huh7 cell and their derivatives)
- Penicillin-streptomycin (100× liquid; Invitrogen, cat. no. 15140-122)
- Nonessential amino acids solution (100×; Invitrogen, cat. no. 11140-050)
- L-glutamine (100×; Invitrogen, cat. no. 25030-081)
- HEPES (1-M solution; Invitrogen, cat. no. 11344-041)
- PBS (–) (see REAGENT SETUP)
- KCl (1-M solution; Sigma, cat. no. 60142)
- KH_2PO_4 (Sigma, cat. no. P9791)
- Methanol (molecular biology grade), 100%
- **Immunofluorescence (IF) buffer** (see REAGENT SETUP)
- Bovine serum albumin (Sigma, cat. no. A2153)
- EDTA (Sigma, cat. no. E5134)
- Antibody to HCV (anti-HCV; e.g., anti–Core C7-50; Affinity BioReagents, cat. no. MA1-080)
- Fluorescent dye–conjugated anti–mouse IgG (Alexa Fluor 488; Invitrogen, cat. no. A11029)

EQUIPMENT

- Agarose gel and apparatus for electrophoresis
- Spectrophotometer (Beckman)
- Electroporation cuvette (0.4-cm gap width; Thermo Hybrid, cat. no. EPECU104)
- Gene Pulser II (Bio-Rad)
- 10-cm culture dish (Corning, cat. no. 430167)
- Bottletop filter unit (0.22-μm PES; Corning, cat. no. 431096)
- Syringe-top disk filter (0.22-μm and 0.45-μm; Millipore, cat. nos. SLGS 033 SS and SLHV 033 RS)
- Amicon Ultra-15 (100,000 NMWL membrane; Millipore, cat. no. UFC9 100 08)
- Poly-D-lysine–coated 96-well plate (Corning, cat. no. 3665)
- Fluorescent microscope

REAGENT SETUP

TE buffer This buffer is 10 mM Tris-HCl, pH 8.0, and 1 mM EDTA, pH 8.0.

ATP solution To prepare, dissolve 0.28 g ATP in 5 ml nuclease-free water. Sterilize with a 0.22-μm syringe-top filter unit.

L-glutathione solution To prepare, dissolve 0.38 g L-glutathione in 5 ml nuclease-free water. Sterilize with a 0.22-μm syringe-top filter unit.

▲ CRITICAL ATP and L-glutathione solutions should be added just before use.

Cytomix buffer Just before use, mix 1 ml cytomix solution, 20 μl ATP solution and 20 μl L-glutathione solution[11]. ▲ CRITICAL Cytomix solution should be prepared so it is RNase free.

Complete medium for cell culture This is low-glucose DMEM containing 10% FBS, 100 U ml^{-1} penicillin, 100 μg ml^{-1} streptomycin, 2 mM L-glutamine, 100 nM nonessential amino acids and 10 mM HEPES. Sterilize with a 0.22-μm bottletop filter unit.

PBS (–) This buffer is 137 mM NaCl, 8.1 mM Na_2HPO_4, 2.68 mM KCl and 1.47 mM KH_2PO_4.

IF buffer This buffer is PBS (–) containing 1% bovine serum albumin and 2.5 mM EDTA.

PROCEDURE

Preparation of template for reverse transcription

1| Obtain the pJFH1 plasmid in appropriate quality and quantity (2 μg μl^{-1}). If necessary, include negative control constructs such as a replication-incompetent construct (pJFH1/GND)[3], an envelop region-deletion construct (pJFH1/ΔE1-E2)[3] or a subgenomic replicon (pSGR-JFH1)[2].

2| Digest pJFH1 DNA with restriction enzymes by combining reagents as follows:

Reagent	Amount
pJFH1 DNA (2 μg μl^{-1})	8 μl (16 μg)
NEBuffer 2 (10x)	5 μl (1× final concentration)
*Xba*I (100 U μl^{-1})	1 μl (100 U)
Nuclease-free water	36 μl
Total volume	50 μl

3| Incubate digestion reactions for 1–2 h in a heat block at 37 °C.

4| Check complete digestion of pJFH1 DNA by separating 0.5 μl of a digested sample, along with the 1 Kb Plus DNA Ladder, by electrophoresis through a 1% agarose gel containing 0.1 μg ml^{-1} ethidium bromide.
? TROUBLESHOOTING

5| Mix the digestion product with 50 μl TE buffer. Pipet into the tube 100 μl phenol–chloroform–isoamyl alcohol (25:24:1 (vol/vol/vol); phenol–chloroform–isoamyl alcohol extraction).

6| Shake vigorously and centrifuge for 15 min at 12,000*g* at 20–25 °C (room temperature).

7| Transfer the aqueous phase to a new tube.

8| Pipet 100 μl chloroform into the tube. Shake vigorously and centrifuge for 5 min at 12,000*g* at room temperature (chloroform extraction).

9| Transfer the aqueous phase to a new tube and pipet 1/10 volume 3 M sodium acetate, 2.5 volume 99.5% ethanol and 1/100 volume glycogen into the tube (ethanol precipitation).

10| Store for 20 min at −80 °C.

11| Centrifuge for 20 min at 12,000*g* and 4 °C.

12| Discard the supernatant and wash the pellet with 500 μl 70% ethanol.

13| Centrifuge for 15 min at 12,000*g* and 4 °C.

14| Discard the supernatant and dry the pellet at room temperature.

15| Resuspend the pellet in 43 μl nuclease-free water.
■ **PAUSE POINT** DNA solution can be stored at −80 °C until further use.

16| Treat with Mung bean nuclease by combining reagents as follows:

Reagent	Amount
Digested DNA solution	43 μl
Mung bean nuclease buffer (10×)	5 μl (1× final concentration)
Mung bean nuclease (10 U μl^{-1})	2 μl (20 U)
Total volume	50 μl

17| Incubate for 30 min in a heat block at 30 °C.

18| Treat with proteinase K by combining reagents as follows:

Reagent	Amount
Mung bean nuclease–treated solution	50 μl
10% (wt/vol) SDS	10 μl
Proteinase K solution (20 μg μl^{-1})	2 μl (40 μg)
Nuclease-free water	138 μl
Total volume	200 μl

19| Incubate for 1 h in a heat block at 50 °C.

20| Extract with 200 μl phenol–chloroform–isoamyl alcohol (25:24:1) as described in Steps 5–7.

21| Extract with 200 μl chloroform as described in Step 8.

22| Precipitate DNA by ethanol precipitation as described in Steps 9–14.

23| Resuspend the pellet in 11 μl nuclease-free water.

24| Pipet 1 μl of the resuspended solution into 49 μl TE buffer (50-fold dilution). Estimate DNA concentration by separating 10 μl of diluted sample, along with a λDNA–*Hin*dIII fragment marker, by electrophoresis through a 1% agarose gel containing 0.1 μg ml^{-1} ethidium bromide.
▲ CRITICAL STEP It is important to confirm the size and yield of the digested DNA fragment.
■ PAUSE POINT DNA solution can be store at −80 °C until further use.
? TROUBLESHOOTING

RNA transcription and purification

25| Transcribe RNA with a MEGAscript kit. First, combine reagents as follows:

Reagent	Amount
Linear template DNA	2–4 μl (500 ng to 1 μg)
ATP solution	2 μl
CTP solution	2 μl
GTP solution	2 μl
UTP solution	2 μl
Reaction buffer (10×)	2 μl
Enzyme mix	2 μl
Nuclease-free water	4–6 μl
Total volume	20 μl

26| Incubate for 3 h in an incubator at 37 °C.

27| Add 1 μl DNase (included in the kit). Incubate for 15 min in an incubator at 37 °C.

28| Add 115 μl nuclease-free water and 15 μl stop solution (included in the kit).

29| Add 100 μl nuclease-free water and purify RNA with 750 μl TRIzol LS according to the instructions of the manufacturer.

30| Resuspend the RNA pellet in 11 μl nuclease-free water.

31| Dilute 1 μl RNA solution with 19 μl nuclease-free water. After denaturing for 5 min at 65 °C, confirm the size of the synthesized RNA by separating 1 μl of diluted sample, along with an RNA ladder, by electrophoresis through a 1% agarose gel containing 0.1 μg ml^{-1} ethidium bromide. Determine the RNA concentration with a spectrophotometer after a further 50-fold dilution (final dilution, 1,000-fold).
▲ CRITICAL STEP It is important to confirm that the size and yield of the purified RNA are appropriate.
■ PAUSE POINT RNA solution can be store at −80 °C for a few months. Avoid repeated cycles of freezing and thawing.
? TROUBLESHOOTING

Transfection (electroporation)

32| Prepare Huh7 cells or the permissive cell lines Huh7.5 or Huh7.5.1. Trypsinize cells and wash with OptiMEM I reduced-serum medium.

33| Resuspend 3.0 × 10^6 cells (for Huh7) or 7.5 × 10^6 cells (for Huh7.5 or Huh7.5.1) with 400 μl Cytomix buffer[11].

34| Mix 10 μg RNA with the 400 μl cell suspension and transfer to an electroporation cuvette.

35| Electroporate the cells with a Gene Pulser II apparatus in conditions of 260 V and 950 μF.

36| Transfer the transfected cells into two 10-cm culture dishes, each containing 8 ml complete medium.

37| Incubate the dishes for 24 h at 37 °C and 5% CO_2.

38| Remove culture medium and wash the transfected cells three times with PBS (−), then add fresh complete medium.

Figure 1 | Infected foci of cell culture–generated HCV-infected cells. Huh 7.5.1 cells were seeded at a density of 1 × 10^4 cells per well in 96-well plates. Each well was inoculated with serially diluted virus solution. At 3 d after infection, inoculated cells were fixed with 100% methanol and were then stained with antibody to core protein (2H9; ref. 3). This image includes six foci. Original magnification, ×200.

39| Transfected cells should be passaged every 2–3 d before the cells become confluent.

Collect the generated HCV

40| Collect culture medium 72 h after transfection and add fresh medium to the cells, then repeat culture medium collection every 2–3 d after cell passage until virus production is decreased.

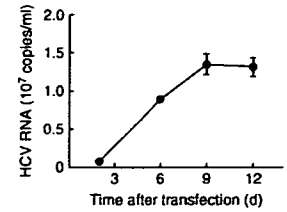

Figure 2 | Transient HCV RNA secretion by transfected Huh7 cells.

41| Remove cell debris by low-speed centrifugation (20 min at 1,000*g*).

42| Pass the culture medium through a 0.45-μm syringe-top filter unit.

43| If necessary, concentrate medium using an Amicon Ultra-15 device. First, pipet filtered culture medium into the Amicon Ultra-15 device (maximum volume is 15 ml). Centrifuge for 30 min at 3,000*g* and 4 °C. Culture medium with virus can be concentrated until the medium reaches 50× concentration.

Titration of generated HCV

44| Check the titer of HCV RNA by quantitative RT-PCR after extracting RNA from medium, as described before[12].
? TROUBLESHOOTING

45| To determine the infectious titer, prepare Huh7, Huh7.5 or Huh7.5.1 cells at a density of 1×10^4 cells per well in poly-D-lysine–coated 96-well plates 24 h before inoculation.

46| Prepare inoculum with serial tenfold dilutions of culture medium containing virus. If a positive control sample is needed, include virus stock solution that has been titrated.

47| Aspirate medium from cells in 96-well plates.

48| Inoculate cells with 100 μl diluted culture medium containing virus. Inoculation of each diluted culture medium should be done in more than triplicate.

49| Incubate the inoculated culture plates for 4 h at 37 °C and 5% CO_2.

50| Remove the inoculum and add 100 μl fresh medium to each well.

51| Incubate the culture plates for 72 h at 37 °C and 5% CO_2.

52| Fix the cells for 20 min at −20 °C with 100% methanol.

53| Incubate the cells for 1 h at room temperature with IF buffer.

54| Incubate the cells for 1 h with anti-HCV at the appropriate concentration (e.g., Anti-Core C7-50, 1:300 dilution).

55| Aspirate the antibody solution and add 100 μl PBS (−) to each well.

56| Aspirate the PBS (−). Repeat Steps 55 and 56 three times (washing step).

57| Incubate the cells for 1 h with fluorescent dye–conjugated anti–mouse IgG at the appropriate concentration (e.g., Alexa 488–anti–mouse IgG, 1:1,000 dilution).

58| Wash cell three times with PBS (−) as in Steps 55–56.

59| Using a fluorescence microscope, select the appropriate well for counting infected foci. In general, the well that was inoculated at the highest dilution among wells showing infectivity should be selected. Count the infected cell foci in the selected well (**Fig. 1**) and multiply the number of infected foci by the dilution factor. The infectious titer is calculated from the average of triplicate procedures.
? TROUBLESHOOTING

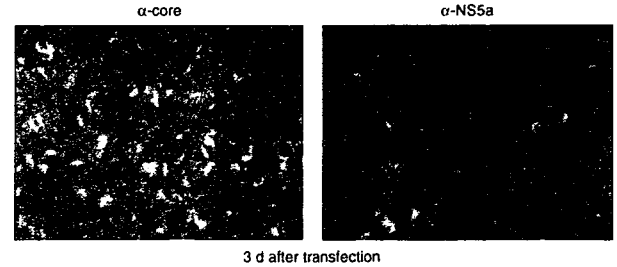

Figure 3 | Immunofluorescence microscopy of HCV proteins in Huh7 cells transfected with JFH-1 RNA. Transfected cells were seeded on coverslips 2 d after transfection, and HCV proteins were detected with antibody to core protein (α-core; 2H9; ref. 3) and to nonstructural protein 5A (α-NS5a; mouse polyclonal serum; ref. 5). Original magnification, ×300.